A numerical investigation of the Mississippi and Atchafalaya freshwater transport, filling and flushing times on the Texas-Louisiana Shelf

Xiaoqian Zhang,[1] Robert D. Hetland,[1] Martinho Marta-Almeida,[1] and Steven F. DiMarco[1]

Received 2 April 2012; revised 3 August 2012; accepted 28 September 2012; published 8 November 2012.

[1] A high-resolution coastal model is used to investigate the transport, filling and flushing times of the freshwater introduced from the Mississippi and Atchafalaya Rivers on the Texas-Louisiana Shelf. The model is forced with realistic forcing, and is nested within hindcasts from the HYCOM operational model. The Mississippi and Atchafalaya discharges are each tagged with dye so that they can be identified and treated separately. The seasonal patterns of freshwater transport are consistent with that expected for the prevailing seasonal winds, but with significant interannual variability. In non-summer months, the major freshwater transport is downcoast and mainly occurs in a narrow band inside of 20-m isobath. In summer, the transport decreases dramatically near the coast due to the competing effects of downcoast buoyancy driven flow and upcoast wind-driven flow. The freshwater transport is upcoast over the mid shelf, in summer, with an offshore component consistent with Ekman transport. We define the shelf domain as the region enclosed by the 100-m isobath, and the along-shore limit of the entire model domain, approximately from the Louisiana-Mississippi border to the Texas-Mexico border. Filling times, based on the river discharge, range from ~3 months (non-summer) to ~6 months (summer) for Mississippi, while for Atchafalaya from ~3–4 months to ~1 year. Flushing times, based on the fresh water flux out of the shelf domain, are more variable, ranging from several months to several years.

Citation: Zhang, X., R. D. Hetland, M. Marta-Almeida, and S. F. DiMarco (2012), A numerical investigation of the Mississippi and Atchafalaya freshwater transport, filling and flushing times on the Texas-Louisiana Shelf, *J. Geophys. Res.*, *117*, C11009, doi:10.1029/2012JC008108.

1. Introduction

1.1. Previous Studies and Goals of This Research

[2] The Texas-Louisiana Shelf is a broad continental shelf with two major fresh water sources, the Mississippi and Atchafalaya Rivers, among several other moderate rivers (e.g., the Brazos River, the Trinity River, and the Sabine River) (Figure 1). The Texas-Louisiana Shelf extends more than 200 km offshore south of Atchafalaya Bay, while it narrows down to less than 50 km near the Mississippi River mouth. The Mississippi River is the largest river in North America and seventh largest river in the world with an average discharge of 20,000 m^3 s^{-1} [*Milliman and Meade*, 1983; *Meade*, 1996]. The Atchafalaya River is a distributary of the Mississippi, and carries one-third of the upper Mississippi River flow; this ratio is controlled by the U.S. Army Corps of Engineers. Both rivers peak in spring. Freshwater inputs onto the shelf play a key role in the formation of bottom hypoxia (oxygen concentrations <1.4 mmol L^{-1}; a level determined to be harmful for marine organisms) over the Louisiana shelf every summer by changing the stratification through altering salinity distributions, as well as carrying an anthropogenicly enhanced nutrient load to the shelf [*Dale et al.*, 2008; *Bianchi et al.*, 2010]. Salinity is the dominant factor affecting stratification over the shelf in summer.

[3] Although the freshwater discharges from the Mississippi and Atchafalaya Rivers play a significant role in shelf dynamics and seasonal shelf hypoxia, relatively few studies have addressed the seasonal patterns of the riverine freshwater distribution, transport, filling and flushing times on the Texas-Louisiana Shelf. In this paper, the *filling time* is defined as the time required to accumulate the freshwater content on the shelf by river discharge. The *flushing time* is defined as the time required to remove the freshwater content on the shelf by integrated amount of freshwater advected off the shelf [*Etter et al.*, 2004]. An early observational study by *Dinnel and Wiseman* [1986] investigated the distribution of the total freshwater content (not only freshwater from rivers) and filling time using a hydrographic data set collected over 1963–1965. According to *Dinnel and Wiseman* [1986], there is an annual

[1]Department of Oceanography, Texas A&M University, College Station, Texas, USA.

Corresponding author: X. Zhang, Department of Oceanography, Texas A&M University, 3146 TAMU, College Station, TX 77843-3146, USA. (zhangxq@tamu.edu)

0148-0227/12/2012JC008108

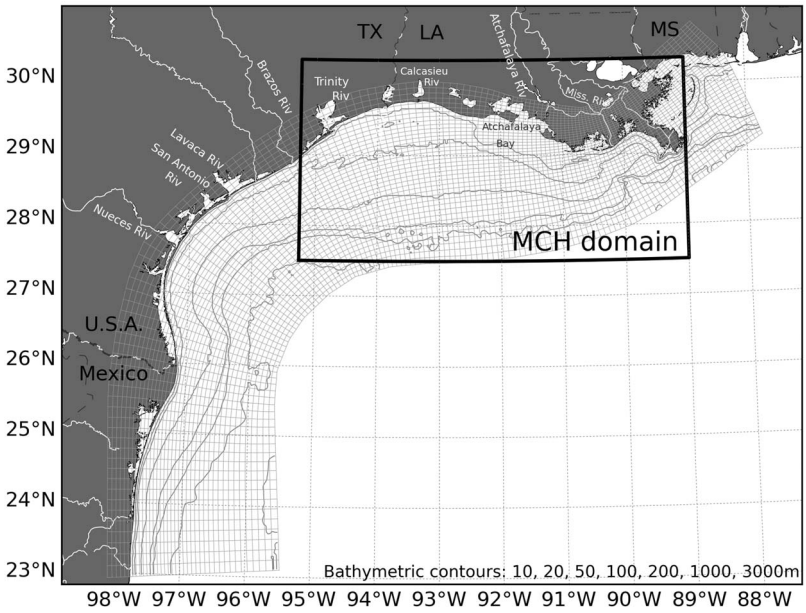

Figure 1. The numerical grid (thin gray squares) is shown in relation to bathymetry (black contours) and the location of geographic features and landmarks. For clarity, only one of five grid points is plotted in the along shore and across shore direction. The rectangular domain represents the region covered by the MCH cruises, and is used in Figure 2 for model salinity validation.

cycle of the freshwater content on the Texas-Louisiana Shelf. They found freshwater volume peaks in summer due to the spring flood, and is lowest in winter. As for the spatial distribution, the highest freshwater content occurs near the coast in winter, while in summer the high freshwater content water may move upcoast (i.e., west to east) and offshore due to a seasonal shift in the winds to upwelling favorable. Filling times exhibit an annual cycle, which is ~3–6 months in spring, and can exceed 1 year in summer when the maximum freshwater volume is present on the shelf [*Dinnel and Wiseman*, 1986]. In a more recent observational study, *Etter et al.* [2004] obtained comparable filling timescales ranging from 4 to 10 months using the data collected on the Texas-Louisiana Shelf during the LATEX project from 1992 to 1994 [*Nowlin et al.*, 1998]. They also estimated the flushing time with the same data set, and found flushing time was on average ~27 days longer than filling time. Freshwater distribution on this shelf has also been investigated using numerical modeling tools. *Morey et al.* [2003] calculated the river discharged freshwater export pathways in the northern Gulf of Mexico (GOM) using a high-resolution numerical model driven by climatological surface and boundary forcings. They found the annual cycle of local wind stress plays an important role in shifting the export pathway of the freshwater discharged from the major rivers. A dominant pathway for cross-shelf export appears near the Mississippi delta throughout the year. However, a second hot spot for cross-shelf transport occurs on the mid-Texas shelf in the summer months.

[4] All three papers provide significant insight to help us understand the distribution and fate of river-associated freshwater on the Texas-Louisiana Shelf. However, there are several limitations in these early studies. The hydrographic data used in *Dinnel and Wiseman* [1986] and *Etter et al.* [2004] are sparse and could not resolve the high-frequency/small scale variability associated with the river plumes. Also, the hydrographic data are not synoptic. The model used by *Morey et al.* [2003] is driven by climatological forcings, and the model results only represent a long-term average. The freshwater content or transport studied in these papers is calculated based on an arbitrary-chosen reference salinity (37 psu in *Dinnel and Wiseman* [1986] and *Etter et al.* [2004]; 36 psu in *Morey et al.* [2003]). Their results may vary if different reference salinity is chosen. Also, these earlier studies treated the Mississippi and Atchafalaya freshwater together.

[5] The goals of this paper are to study the transport, filling and flushing times of the Mississippi and Atchafalaya freshwater separately, using a high-resolution (~1 km) coastal model of Texas-Louisiana Shelf. The model is forced with realistic surface momentum, heat, salt fluxes and open boundary conditions. The simulation is carried out from 2003 to 2010 so that we can look at the interannual variability associated with the riverine freshwater. A particular advantage of the present modeling approach is that the freshwater from each river is tagged with a dye so that we can identify riverine water precisely, and treat each river individually. Since each dye represents the concentration of freshwater from one river, we avoid choosing the somewhat arbitrary reference salinity to calculate the concentration as has been done in the early studies [*Dinnel and Wiseman*, 1986; *Etter et al.*, 2004; *Morey et al.*, 2003].

1.2. Circulation on the Texas-Louisiana Shelf

[6] In terms of circulation, the Texas-Louisiana Shelf may be approximately divided into an inner and outer shelf by the 50 m isobath. Wind-driven circulation dominates the inner shelf, whereas interaction with Loop Current Eddies

influences the outer shelf [*Nowlin et al.*, 2005; *Ohlmann et al.*, 2001]. *Cochrane and Kelly* [1986] and *Cho et al.* [1998] described the seasonal wind-driven circulation over the inner shelf. In the summer months, when winds are weakly upwelling favorable, fresh water tends to collect on the eastern shelf, and thus intensify the local stratification. During winter, the winds reverse to downwelling favorable, enhancing downcoast flow of fresh water, and with the addition of frontal passages that mix the water column, the stratification created in summer is reduced. This seasonal pattern is modulated between years by changes in prevailing winds and the magnitude of the fresh water discharge, and it affects important shelf processes: transport of harmful algae blooms, nutrient cycling, and seasonal hypoxia [*Hetland and Campbell*, 2007; *Hetland and DiMarco*, 2008; *Wang and Justic*, 2009; *DiMarco et al.*, 2010; *Bianchi et al.*, 2010]. As for shorter time scales of hours to days, the circulation on this shelf is mainly driven by land/sea breeze especially during summer months. Land/sea breeze can drive significant near-inertial currents because of the coincidence of the period of land/sea breeze ($\sim$1 day) and the inertial period of the ocean ($\sim$1 day) [*DiMarco et al.*, 2000; *Zhang et al.*, 2009, 2010]. These near-inertial currents represent the strongest non-storm induced currents on this shelf, and can reach more than 60 cm s^{-1}.

2. Hydrodynamic Model Configuration

[7] In this paper, we will use the results from a high-resolution model from 2005 to 2010 to quantify the river-discharged freshwater distribution, transport, filling and flushing times on the Texas-Louisiana Shelf. Both multiple year average and interannual variability will be addressed.

[8] The simulations were performed using the Regional Ocean Modeling System (ROMS, 3.4). ROMS is a free-surface and terrain-following hydrodynamic ocean model widely used by the scientific community for a diverse range of applications [*Haidvogel et al.*, 2000; *Shchepetkin and McWilliams*, 2005]. The model domain covers the entire Texas-Louisiana shelf and slope area (Figure 1), with a resolution of $\sim$500 m near the coast, and $\sim$1–2 km on the outer slope area. The model has 30 vertical layers with a minimum water depth of 3 m, and a maximum water depth greater than 3000 m (realistic topography). The model is configured to use recursive multidimensional positive definite advection transport algorithm for horizontal advection of tracers, third order upwind advection of momentum, conservative splines to calculate vertical gradient, and *Mellor and Yamada* [1974] turbulence closure with the *Galperin et al.* [1988] stability functions.

[9] The Texas-Louisiana Shelf model was initialized on Feb 1, 2003, with the initial and open boundary conditions provided by the Gulf of Mexico Hybrid Coordinate Ocean Model (GOM-HYCOM) (http://www.hycom.org). GOM-HYCOM is a hybrid isopycnal-sigma-pressure coordinate ocean model. The model domain includes the entire Gulf of Mexico. The horizontal resolution is 1/25 degree and it has 20 vertical levels. HYCOM possesses the advantages of the different vertical discretizations to simulate from shallow coastal features to large scale open-ocean circulation. The hybrid vertical discretization dynamic transitions between the different coordinates: isopycnal in the open, stratified ocean, terrain-following in coastal regions and constant z-level coordinates in unstratified areas, like the surface mixed layer. The HYCOM nowcast/forecast system runs are available in real time from the Naval Oceanographic Office (NAVOCEANO). Surface atmospheric forcing is provided by the Navy Operational Global Atmospheric Prediction System (NOGAPS). HYCOM assimilates data from several sources, including along-track satellite altimetry observations, satellite-measured and in situ surface temperature, and vertical temperature profiles from XBTs, ARGO and moored buoys. Assimilations are done with the Navy Coupled Ocean Data Assimilation system (NCODA). The GOM-HYCOM implementation is nested in the Atlantic scale 1/12 HYCOM model. The model outputs are available as daily snapshots at standard Levitus depth levels.

[10] At the three open boundaries (south, east, west), a nudging layer of six cells was used to relax the model temperature, salinity and baroclinic velocities toward HYCOM. The nudging time scale used was eight hours at the boundaries with a sinusoidal decay to the interior. Radiation conditions [*Marchesiello et al.*, 2003] were used at the boundaries for tracers and baroclinic velocities. Sea surface height and barotropic currents from HYCOM were imposed at the boundaries as *Chapman* [1985] and *Flather* [1976] boundary conditions. For a description of the advantages of this nesting approach see *Barth et al.* [2008].

[11] The hindcast Texas-Louisiana Shelf model is forced with 2-d wind, and sea surface heat and salt fluxes from the North American Regional Reanalysis (NARR) data set. The NARR forcing has 3-h temporal resolution and 32 km spatial resolution. Long wave radiation, latent, and sensible heat fluxes are calculated in ROMS internally. Because the surface heat flux is only prescribed as a boundary condition, there is no feedback from the ocean to the atmosphere heat flux forcing such that drifts in SST occur due to small but persistent errors in heat flux. To correct for this, a uniform Q-correction of 50 Watts/m^2/°C is used to relax the sea surface temperature to spatially uniform monthly sea surface temperature climatology. Fresh water fluxes from the Mississippi and Atchafalaya Rivers are specified using daily measurements of Mississippi River Transport at Tarbert Landing by the U.S. Army Corps of Engineers. Fresh water fluxes from the other seven rivers (the Nueces, San Antonio, Lavaca, Brazos, Trinity, Sabine, Calcasieu Rivers) are prepared based on the USGS (U.S. Geological Survey) Real-Time Water Data for the Nation.

[12] To track the freshwater from major rivers, the Mississippi and Atchafalaya discharges are each tagged with a dye. Each dye has a value between 0 and 1, and represents the concentration of the corresponding river freshwater, i.e., if dye has a value of 1, it means the water parcel is purely river water; if dye has a value of 0, it means the water parcel contains no freshwater from that river. The governing equations for dye are the same as other tracers (e.g., temperature and salinity), and can be found at the ROMS website (https://www.myroms.org/wiki/index.php/Equations_of_Motion). At the open boundaries, the dyes are nudged to the ocean water (dye is equal to zero) in the same manner as temperature and salinity. Tides are not included in the model, but are known to be small in the region [*DiMarco and Reid*, 1998]. The model simulation is run for $\sim$eight years from 2003 to

Table 1. Research Cruises for the Mechanisms Controlling Hypoxia (MCH) Project During Years 2004–2008[a]

Hypoxia Cruise	Time	Research Vessel	Number of CTD Profiles
2004 MCH01	2–8 April 2004	R/V Gyre	57
2004 MCH02	25 June–1 July 2004	R/V Gyre	60
2004 MCH03	20–27 August 2004	R/V Gyre	63
2005 MCH04	23–29 March 2005	R/V Gyre	104
2005 MCH05	20–26 May 2005	R/V Gyre	102
2005 MCH06	8–14 July 2005	R/V Gyre	142
2005 MCH07	18–24 August 2005	R/V Gyre	231
2007 MCH08	22–29 March 2007	R/V Pelican	225
2007 MCH09	17–20 July 2007	R/V Pelican	110
2007 MCH10	6–9 Sep 2007	R/V Pelican	139
2008 MCH11	16–19 April 2008	R/V Pelican	43
2008 MCH12	17–20 July 2008	R/V Pelican	71

[a]Over 1300 salinity profiles were collected during these cruises, and these salinity data were used for model validation.

2010. It takes about five days to integrate the simulation for one year on a supercomputer using 512 processors.

3. Model Skill Assessment

[13] A manuscript that is dedicated to the development and validation of the Texas-Louisiana Shelf model has been published [*Zhang et al.*, 2012]. In that work, the skill of the Texas-Louisiana Shelf model output was evaluated using extensive measurements collected in this region during the simulation period. These include current and temperature comparisons with measurements from the Texas Automated Buoy System (TABS), sea surface height comparisons with measurements from the Texas Coastal Ocean Observation Network (TCOON), and AVISO (satellite altimetry). These comparisons over multiple years show that the model is able to reproduce realistic currents, sea surface height, and temperature on the Texas-Louisiana Shelf [*Zhang et al.*, 2012].

[14] *Zhang et al.* [2012] did not address the validity of the modeled salinity field. Because the goals of this paper are to study the river discharged freshwater transport, its associated filling and flushing times, it is key to assess the model's ability to simulate the salinity field correctly. In this paper, we will use ~1300 salinity profiles collected on the Texas-Louisiana Shelf during the 12 Mechanisms Controlling Hypoxia (MCH) hydrographic cruises from 2004 to 2008 to validate the salinity field. The approach used here for our assessment of the salinity field is similar to *Hetland and DiMarco* [2012]. The MCH cruises were organized in a number of clustered stations mainly between 10 and 100 m deep along the shelf. For model validation of other variables, please refer to *Zhang et al.* [2012].

3.1. Hydrography

[15] Observational data presented here were collected aboard the *R/Vs Gyre* and *Pelican* during 12 MCH cruises from 2004 to 2008 (Table 1). Vertical profiles of salinity and temperature were made using a Seabird SBE 911 CTD. Continuous measurements of salinity and temperature were made using a thermosalinograph with water intake located in the ship's bow and at about 3 m depth. All hydrographic sensors were periodically factory calibrated to mitigate long-term sensor drift. Water samples were analyzed using a Guildline salinometer and compared to the conductivity derived salinity estimates from the CTD and thermosalinograph. The comparison showed agreement that was within acceptable tolerances for coastal research (i.e., usually within 0.1 psu).

3.2. Model Skill

[16] In this study, we use both the non-dimensional model skill and dimensional root-mean-square (RMS) to quantify the ability of the model to reproduce observed salinity. A similar method has been applied in earlier research to evaluate models in other regions [e.g., *Warner et al.*, 2005; *Liu et al.*, 2009]. The skill used in this study is defined as

$$skill = 1 - \frac{\sum_{i=1}^{N} (d_i - \Im[m_i])^2}{\sum_{i=1}^{N} (d_i - c_i)^2} \quad (1)$$

where d_i are the available measurements, and $\Im[m_i]$ is a row vector of the model results in which m_i is transformed by the linear operator $\Im$ to match the measurements, c_i is a vector of climatological values [*Bogden et al.*, 1996; *Hetland*, 2006]. The climatological values c_i for salinity are from the World Ocean Atlas 2009 (WOA09) [*Johnson et al.*, 2009]. WOA09 is a set of objectively analyzed ($1^\circ \times 1^\circ$ resolution) climatological fields (e.g., temperature, salinity and dissolved oxygen) based on in situ measurements. Detailed information about WOA09 can be found at the National Oceanographic Data Center (NODC) website (http://www.nodc.noaa.gov/OC5/WOA09/). When estimating the model skill for salinity, both the model output and climatology were interpolated to the profile locations. The RMS of observation relative to model and climatology are defined as

$$(Obs - Mod)_{RMS} = \sqrt{\frac{\sum_{1}^{N} (d_i - \Im[m_i])^2}{N}}, \quad (2)$$

and

$$(Obs - C\,\mathrm{lim})_{RMS} = \sqrt{\frac{\sum_{1}^{N} (d_i - c_i)^2}{N}}, \quad (3)$$

respectively.

[17] For a perfect model that reproduces the observations exactly, the model skill is one. If the RMS of the model error (d-m), is equal to the RMS of the data relative to the climatology (d-c), the skill is zero. It is possible to have a negative skill if the model error variance is larger than the data variance, that is if the model actively disagrees with observed values. This model skill evaluates model performance based on climatology. A positive skill indicates that the model can reproduce more variance in the data than climatology, while a negative skill means less. *Hetland* [2006] provides a detailed description of the possible interpretations of model skill under a number of different conditions.

3.3. Comparisons With Hydrography

[18] Figure 2 shows the skill of the model in predicting salinity over the upper 50 m of the water column based on the MCH hydrographic observations. All profiles are interpolated to 1 m vertical intervals prior to the calculation. Positive (red) values of normalized model error indicate that

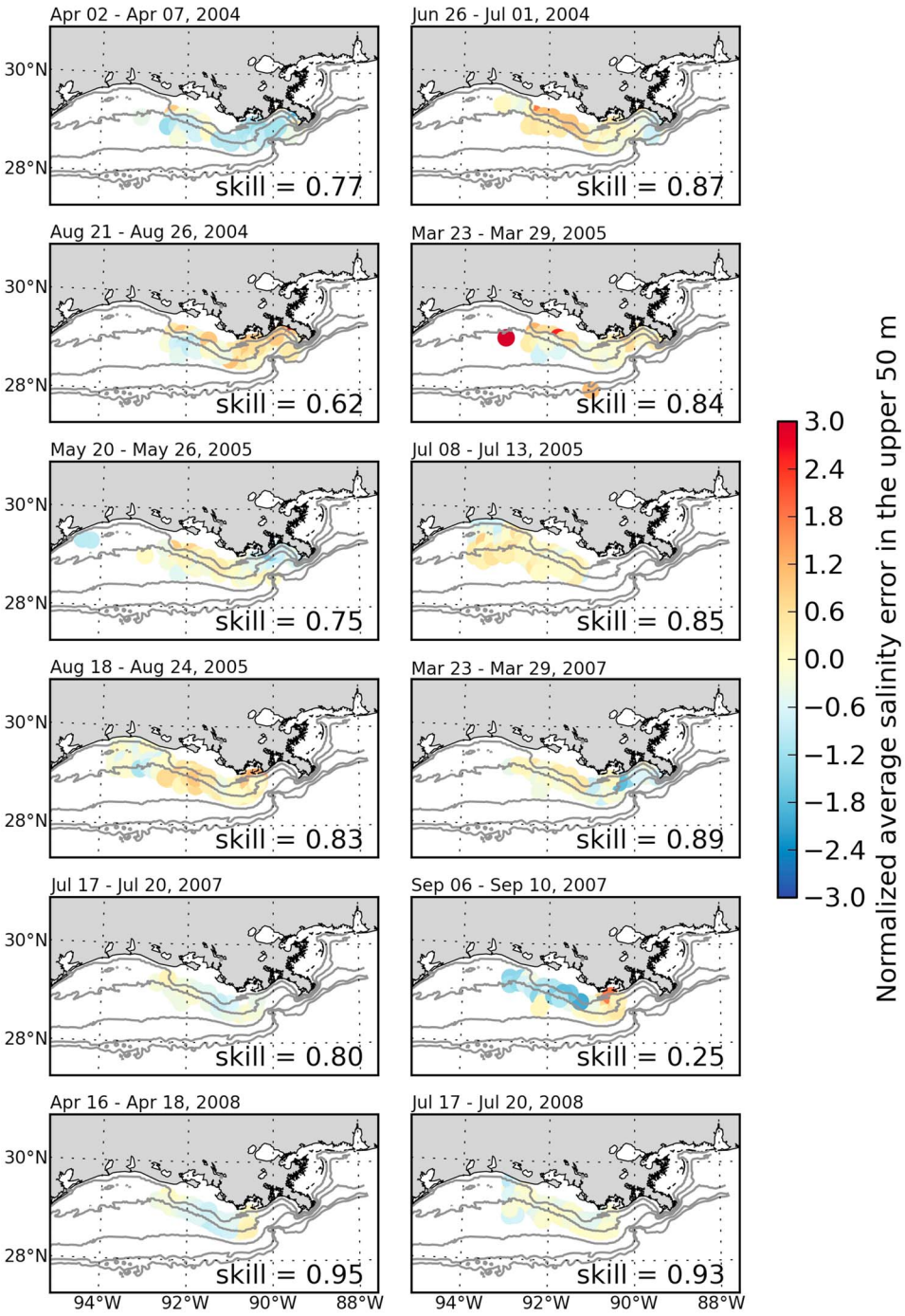

Figure 2. Each panel shows the error in predicted salinity for twelve shelf-wide cruises (part of the Mechanisms Controlling Hypoxia field program) averaged over the upper 50 m of the water column, normalized by the RMS of the observed salinity relative to climatological salinity. The cruise dates and model skill are also shown for each cruise. The number of salinity profiles used for each cruise is shown in Table 1.

the simulated upper layer average salinity is saltier than measured, negative (blue) values are fresher. The skill is calculated for each cruise using point-by-point comparisons over the upper 50 m of the water column. The skill is positive in all cases, indicating that the model is a more accurate representation of the observations than the climatology. The skill is typically larger than 0.6, indicating that the model reproduces about 60% more variance beyond that already described by the seasonal climatology. The error is more or less randomly distributed in space, and predicted salinity is higher at some stations and lower at others. These patterns of errors may be associated with misrepresentation of the meso-scale eddies in our model (Figure 2). Energetic eddies on the order of 50 km have been observed in this region, which are

Table 2. Root-Mean-Square (RMS) of the Observed Salinity Relative to Modeled Salinity and Climatological Salinity, Respectively (Equations (2) and (3)) for Each Hypoxia Cruise During Years 2004 to 2008

Hypoxia Cruise	RMS (Obs − Mod)	RMS (Obs − Clim)
2004 MCH01	1.61	3.33
2004 MCH02	1.24	3.38
2004 MCH03	1.52	2.47
2005 MCH04	1.52	3.79
2005 MCH05	1.69	3.42
2005 MCH06	1.29	3.35
2005 MCH07	1.40	3.42
2007 MCH08	1.44	4.38
2007 MCH09	1.56	3.51
2007 MCH10	1.65	1.90
2008 MCH11	1.39	6.13
2008 MCH12	1.36	5.00

caused by the nonlinear interaction of river plume and bathymetric structures [*DiMarco et al.*, 2010] and modeling study suggested that these eddies are hard to simulate because they can be chaotic due to nonlinearity [*Hetland and DiMarco*, 2012; M. Marta-Almeida et al., Evaluation of model nesting performance on the Texas-Louisiana continental shelf, submitted to *Journal of Geophysical Research*, 2012].

[19] The smallest model skill (0.25) occurs for the September cruise in 2007 (Figure 2). This is because the salinity observations are close to climatology during that cruise. We calculated the dimensional RMS of observations relative to model and climatology for each cruise (Table 2). From Table 2, we can see the smallest $(Obs - Clim)_{RMS}$ (1.90) occurs for the September 2007 cruise. Therefore, a small denominator in equation (1) causes a small skill even though the model error is comparable to other cruises (Table 2). This indicates, for this cruise, much of the variability in the salinity measurements has already been captured by climatology. However, a skill of 0.25 means the model is able to reproduce 25% more variance than those already described in climatology.

[20] Figure 3 shows error histograms for salinity simulation, this time over the entire profile depths. The histogram represents point-by-point model error, normalized by the RMS of the observation relative to the climatology over a particular cruise. To gain some insight into the cross-shore structure of the model error, the normalized error is separated into three bathymetric ranges: 0–20 m, 20–50 m, and 50–200 m.

[21] From Figure 3, we can see the model is able to reproduce the observed salinity especially at the deep stations. The deeper water masses, hydrographic stations taken in water depths between 50 and 200 m, show small bias and less than a standard deviation in the normalized spread in the errors. Error histograms in shallower water are broader, and show occasional bias (e.g., September 2007), particularly in stations taken in water shallower than 20 m. The model error is seldom normally distributed, as assumed by most modern data assimilation techniques. Rather, there are fairly large biased sections of the shelf that contribute to distinct secondary side lobes in almost all of the hydrographic comparisons. Thus, the spread in the Gaussian section of the error represents errors that are unresolvable by the model. It would most likely be possible to correct for the larger-scale water mass biases represented by the secondary off-center peaks.

[22] The comparisons between model-simulated and observed salinity indicate the model simulates a realistic salinity field on the Texas-Louisiana Shelf (thus the far-field plume structure). Since we notice it takes about two years for the salinity field to reach equilibrium (salt content on the Texas-Louisiana Shelf becomes stable) in our domain, we exclude the first two-year simulation results (2003 and 2004) in the following analysis. We study the characteristics of distribution, transport, filling and flushing times of the Mississippi and Atchafalaya discharged freshwaters on the Texas-Louisiana Shelf using the model results from 2005 to 2010.

4. Results

4.1. Climatological and Interannual Variability of Freshwater Thickness and Vertically Integrated Freshwater Transport

[23] In order to study the spatial distribution of the freshwater, we use the freshwater thickness h, which is defined as

$$h_m(x,y,t) = \int_{-H}^{0} dye_m(x,y,z,t)dz, \tag{4}$$

where x, y, z, and t are along-shore, across-shore, vertical and time variables respectively. Dye is the river water concentration, m is the dye index (1 is for Mississippi, and 2 is for Atchafalaya), and H is the total water depth. The physical explanation of the freshwater thickness is the thickness of a freshwater layer if we 'unmix' the water column such that all the freshwater lies on top of pure ocean water. For the dye thickness, h_m, it is the fresh water associated only with one source.

[24] The vertically integrated freshwater transport for each river is defined as

$$\vec{Q}_m(x,y,t) = \int_{-H}^{0} \vec{u}\ dye_m(x,y,z,t)dz, \tag{5}$$

where $\vec{Q}_m$ is the transport, and $\vec{u}$ is the vector velocity. $\vec{Q}_m$ can be treated as the volume transport normalized by the grid length (dx or dy). In this study, we examine both the climatological (average over years 2005–2010) and interannual variability of the monthly mean freshwater thickness and vertically integrated transport for Mississippi and Atchafalaya, respectively.

[25] Figure 4 shows the climatological monthly mean Mississippi freshwater thickness and transport on the Texas-Louisiana Shelf. The majority of the freshwater stays inside of 50-m isobath throughout the year. Typical Mississippi freshwater thickness is on the order of 1 m, although it can reach 3 m near the river mouth. The freshwater thickness decreases dramatically to <0.1 m seaward of the 50 m isobath. The Mississippi freshwater can reach the western boundary of the model domain (~23°N) in the non-summer months due to downwelling favorable winds, while in July and August the freshwater is pooled on the Texas-Louisiana Shelf and the southern edge of the freshwater stays on the

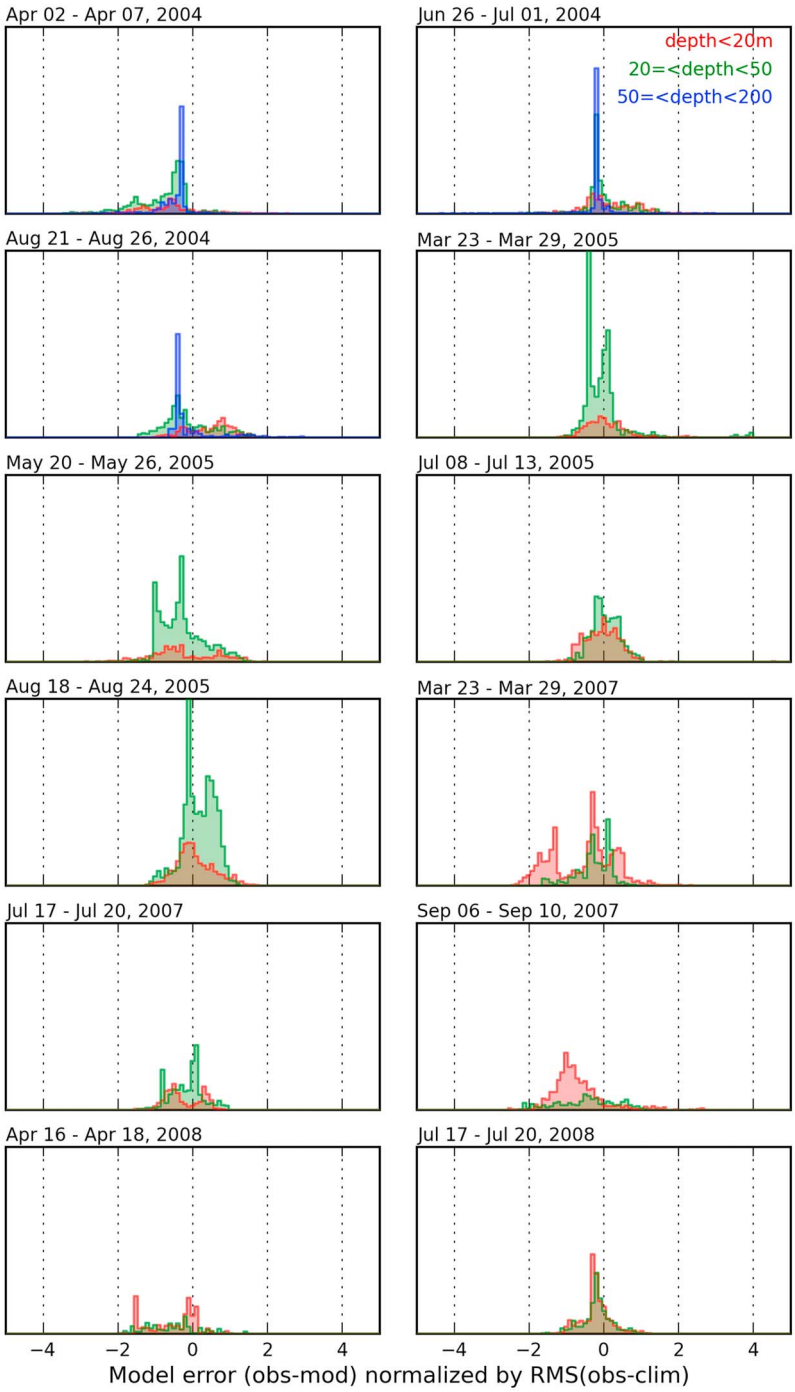

Figure 3. These histograms show the normalized model error in predicting salinity from hydrographic measurements during the MCH program. Histograms are normalized by the RMS of the observed salinity relative to climatological salinity. The histogram is shaded by the three bathymetric ranges: 0–20 m (red), 20–50 m (green), and 50–200 m (blue). Note: the stations during the 2005–2008 cruises are all inshore of 50-m isobaths.

Texas shelf (~26°N) because of upwelling favorable winds (Figure 4).

[26] The vectors in Figure 4 show the climatological monthly mean depth-integrated Mississippi freshwater transport in our domain. One feature shown in this figure is that the maximum freshwater transport occurs to the west of the Mississippi delta between 89°W and 90°W (a region known as the Louisiana Bight). The freshwater transport can reach 0.6 $m^2 s^{-1}$ in magnitude due to the combined effect of the following three reasons. First, Mississippi river freshwater thickness is maximum (Figure 4). Second, a semi-persistent meso-scale gyre stays in this region throughout the year; currents within this gyre are strong [*Ichiye*, 1960], and

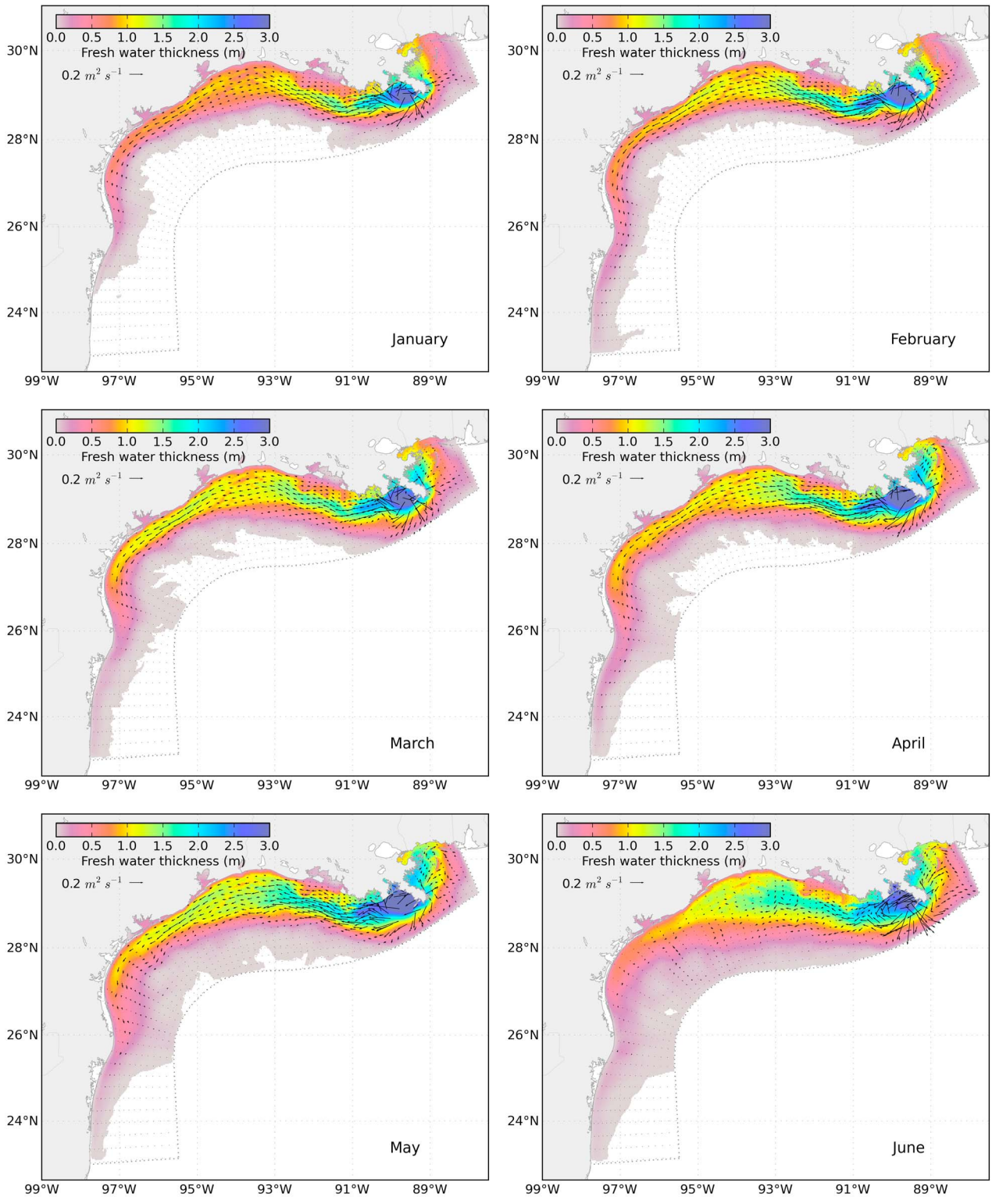

Figure 4. Model multiple-year average (2005–2010) of Mississippi River freshwater thickness and transport in the study region. The colors represent the spatial distribution of Mississippi freshwater thickness. The arrows represent the freshwater transport.

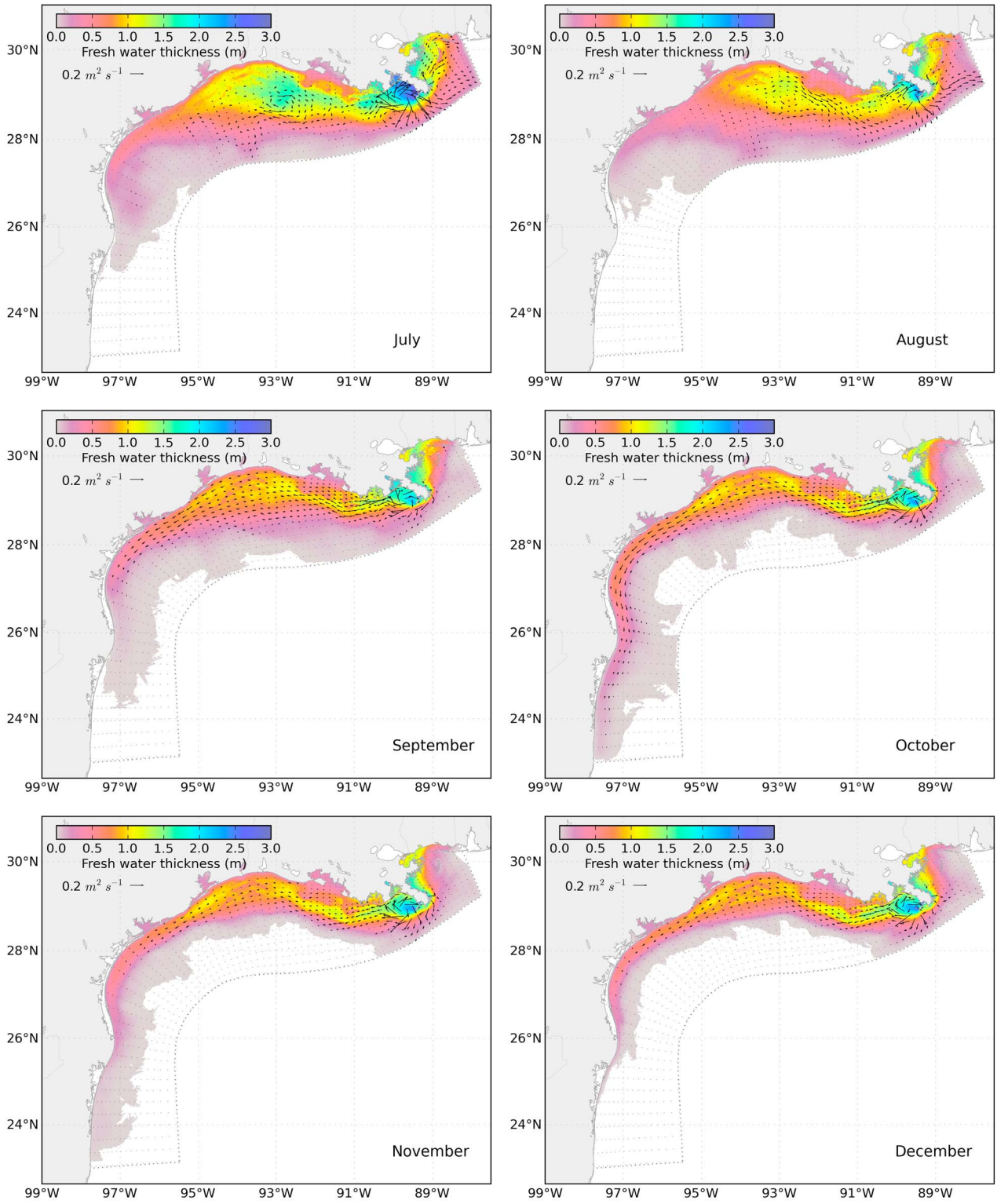

Figure 4. (continued)

can reach 1 m s^{-1} (not shown). Third, the bathymetry is steep, and the continental shelf is narrow in this region.

[27] Aside from the maximum values associated with the meso-scale gyre near the river mouth, the Mississippi climatological monthly mean freshwater transport displays similar pattern as that of the Mississippi freshwater thickness (Figure 4). In the non-summer months, the major freshwater transport is downcoast and occurs mainly in a narrow band

inshore of the 20 m isobath. Maximum transport is ~0.2 m^2 s^{-1}, which occurs between 10- and 20-m isobaths on the Louisiana shelf. Freshwater transport drops significantly seaward of the 50-m isobath on the Texas-Louisiana Shelf. Non-summer freshwater transport is larger in winter and spring than in fall (Figure 4). In summer, the transport decreases dramatically near the coast due to the competing effect of downcoast-propagating freshwater and upcoast wind (Figure 4). The freshwater transport is upcoast on the mid shelf with significant offshore component, consistent with the Ekman transport driven by the upcoast wind in the northern hemisphere. Figure 4 also shows the climatological maximum offshore transport occurs on the mid Louisiana Shelf in July and August, and it reaches ~0.1 m^2 s^{-1}.

[28] The climatological freshwater thickness and transport for Atchafalaya River display generally similar patterns as those for Mississippi, but with a couple of notable differences (Figure 5). First, Atchafalaya freshwater lies in a narrower band hugging the coast, while Mississippi plume is wider. In the region near the Atchafalaya delta, the majority of freshwater comes from Atchafalaya because the Mississippi discharge tends to stay seaward of the 10-m isobath. This is due in part to the momentum of the Atchafalaya as it enters the shelf and flushes the shallow waters (comparing freshwater thickness between Figures 4 and 5). Second, little freshwater from Atchafalaya goes upcoast toward the Mississippi delta in the non-summer months. Consequently, there is almost no interaction in the non-summer months between Atchafalaya freshwater and the Loop Current since the Loop Current effect is most dominant near the Mississippi delta. In the summer months, upcoast wind can bring the Atchafalaya water to the bird-foot of Mississippi delta, where it can interact directly with the Loop Current.

[29] In order to examine the interannual variability on the Texas-Louisiana Shelf, we plot the July–averaged Mississippi and Atchafalaya freshwater thickness and transport for each individual year in Figures 6 and 7, respectively. July is chosen because this is the month of particular interest in this region when the prevailing wind have reversed to upcoast, freshwater pools on the shelf, and coastal hypoxia is considered strongest. From Figure 6, we can see significant interannual variability of Mississippi freshwater thickness and transport from 2005 to 2010, which is caused by the interannual variability of the wind-forcing and river discharge. For example, the Mississippi water was pushed further downcoast to ~25°N in July in years 2005 and 2007 when the upcoast wind was weaker and persisted shorter. In contrast, when the upcoast wind was stronger and lasted longer in years 2006, 2008, and 2009, Mississippi freshwater was constrained to the north of ~27°N (Figure 6). In particular, 2009 is a special year when upcoast wind was stronger, and persisted much longer than climatology. The observed hypoxic area in July 2009 is much smaller as contrast to what is expected based on the flooding of Mississippi river in that year [*Forrest et al.*, 2011]. This is partially caused by the significant offshore freshwater transport by the strong upcoast wind in 2009 (Figure 6), which lasted for nearly one and a half months [*Feng et al.*, 2012]. In other words, although river discharge was very large in 2009, persistent upcoast wind was efficient in removing the freshwater on the Texas-Louisiana Shelf to the open ocean. As a result, freshwater thickness on the Texas-Louisiana Shelf in 2009 was shallower comparing to 2008 (Figure 6), when freshwater discharges were also very large and comparable. In 2008, summer hypoxia was widespread and extended from the Mississippi River delta to Corpus Christi, TX (http://www.ncddc.noaa.gov/hypoxia/).

[30] The year 2009 is an extreme example, but a similar process acts in all years. Figure 6 also indicates that offshore transport is weaker in other years (e.g., 2005) when the upcoast wind is weaker and not persistent. Because of this, there is a significant correlation between not only river discharge and hypoxia (a result of buoyancy forcing and nutrient loading) but also between hypoxic area and the magnitude [*Forrest et al.*, 2011] and duration [*Feng et al.*, 2012] of east-west wind stress on the shelf. Another feature shown in Figure 6 is the meso-scale eddies with the horizontal scale of 50–100 km on the mid Texas-Louisiana Shelf (away from the Mississippi delta; e.g., near 92.5°W, 29°N in July 2008 case).

4.2. Hot Spots for Offshore Transport

[31] Since there is large amount of river freshwater that is discharged to the Texas-Louisiana Shelf every year, it is important to know where the freshwater leaves the Texas-Louisiana Shelf. In order to quantify this, we define the Texas-Louisiana Shelf as the region enclosed by the 100-m isobath (Figure 8). The along-isobath distance is also labeled in Figure 8, and the boundary between Texas and Louisiana coastal waters lies roughly around 800 km. The model-simulated velocity and dye information are interpolated to the 100-m isobath and the vertically integrated transport perpendicular to the isobath is then calculated. The transport calculations are averaged over a 2-week period to remove short-duration fluctuations.

[32] Figure 9a shows the distribution of the offshore vertically integrated freshwater transport for Mississippi as a function of time and along-isobath distance. From Figure 9, we can see there is strong offshore transport near the location of 1300 km throughout 2005 to 2010. The magnitude is between 0.21 m^2 s^{-1} and 0.28 m^2 s^{-1}. This location is consistent with the eastern edge of the semi-persistent meso-scale eddy residing near the mouth of the Mississippi River (Figure 4). The outflow in this region was strongest in 2008 while smaller in 2006 and 2007 (Figure 9). The year 2008 was a flooding year for the Mississippi and the model results indicate that there was stronger interaction between the river-discharged freshwater and the meso-scale eddy in that year.

[33] There are two other hot spots for the offshore transport (Figure 9). One lies on the Texas shelf (between 300 km and 800 km) and the other on the Louisiana shelf (between 900 km and 1200 km). These two hot spots for offshore transport both have maximum values of ~0.20 m^2 s^{-1}, and occur mainly during the summer months (Figure 9). The offshore transport also displays significant interannual variability. The hot spot on the Texas shelf is seen in all the years except 2006 (a low discharge year), while that on the Louisiana shelf is more apparent from 2008 to 2010. Also, it is interesting to note that the summer hot spots on the Texas shelf propagate upcoast (from Texas toward Louisiana) with time; they lie between 400 km and 600 km in May and June, and move to between 600 km and 800 km in July and August (Figure 9). In contrast, the hot spots on the Louisiana

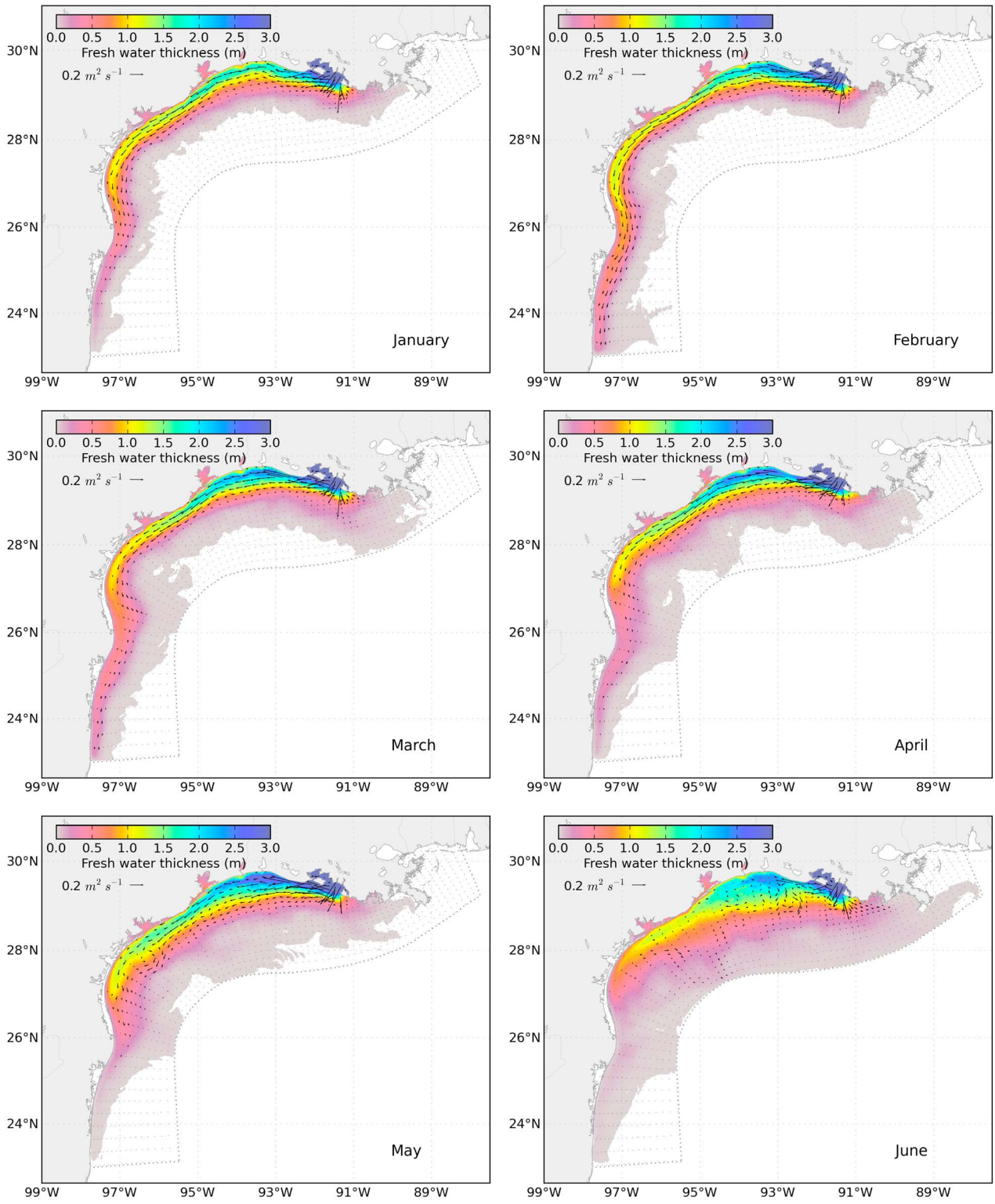

Figure 5. Same as Figure 4 but for Atchafalaya freshwater.

shelf seem to be more stationary. The propagation of the hot spots on the Texas shelf can be explained by the shifting wind that drives the freshwater upcoast in summer. Consequently, the hot spots for offshore transport on the Texas shelf move upcoast. The two hot spots coincide with kinetic energy maxima locations of the shelf edge [*Nowlin et al.*, 2005].

[34] The Mississippi inflow is also shown in Figure 9b. The inflow is smaller compared to the outflow, and displays

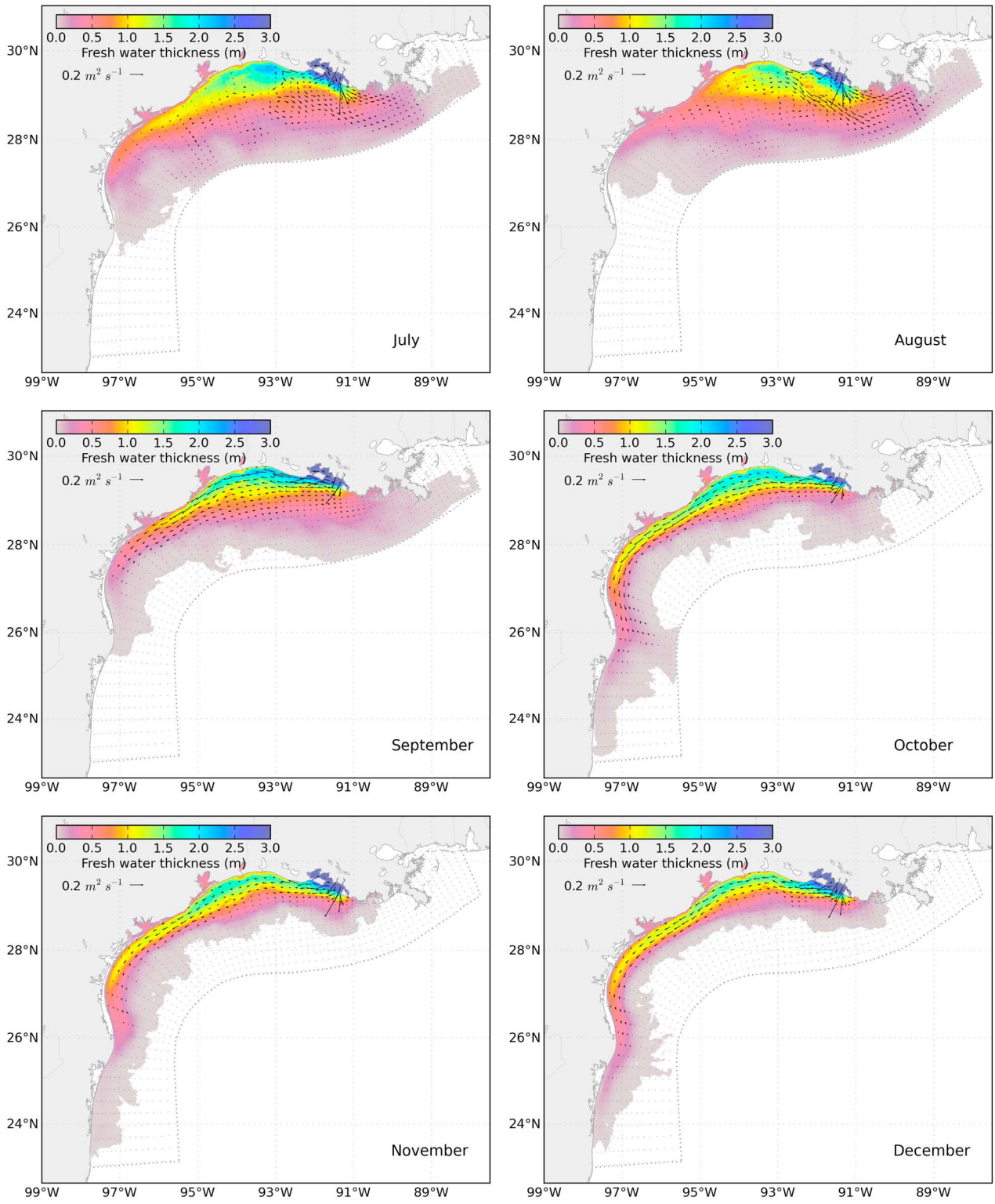

Figure 5. (continued)

less variability. One feature shown in Figure 9 is the significant inflow near 1200 km. The maximum inflow is between 0.14 $m^2\ s^{-1}$ and 0.21 $m^2\ s^{-1}$. This location is consistent with the western edge of the meso-scale eddy residing near the river mouth (Figure 4). Comparisons of inflow and outflow in Figure 9 show that this anticyclone eddy pushes Mississippi freshwater offshore near the eastern edge and bring part of it back near the western edge.

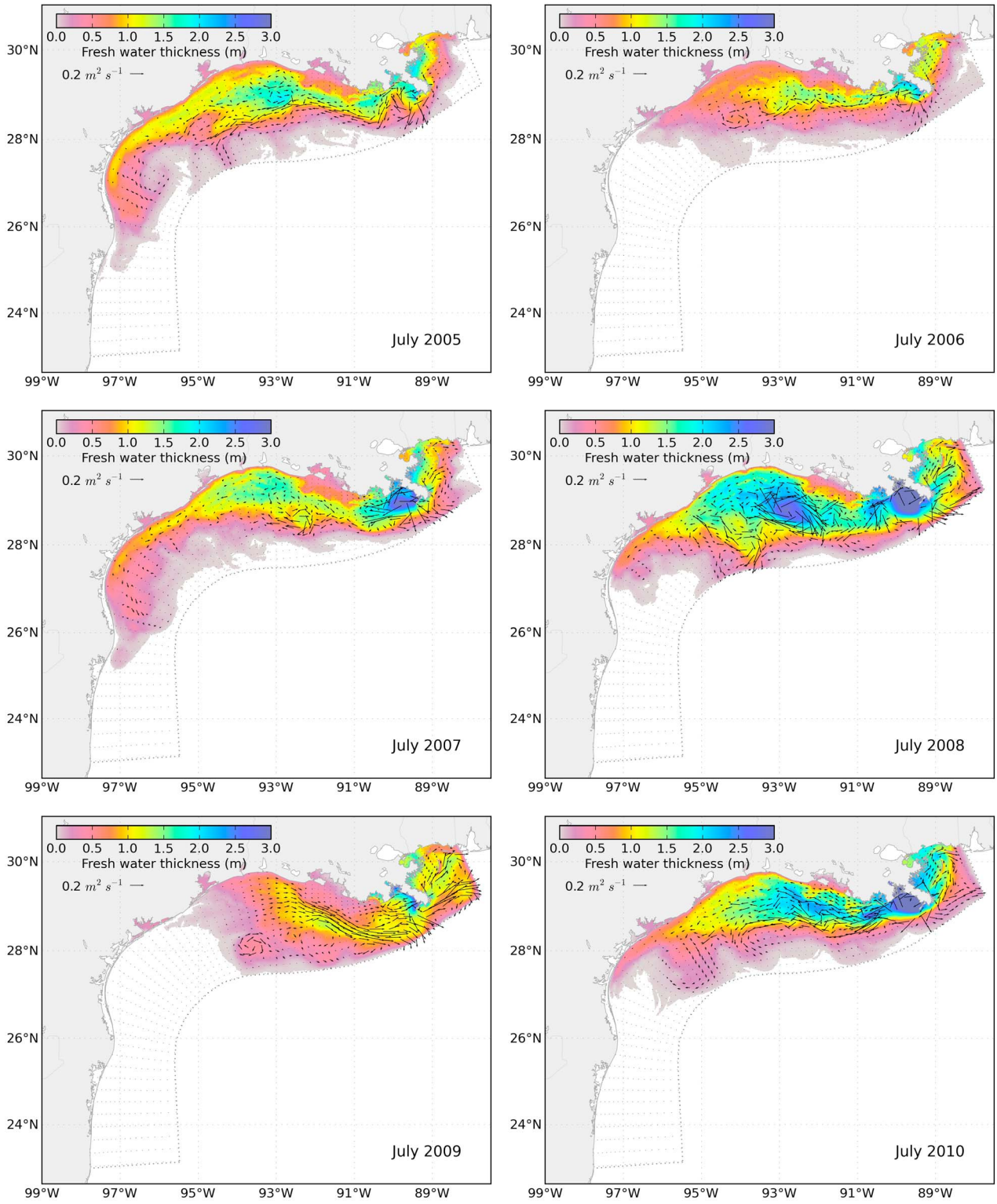

Figure 6. Interannual variability (2005–2010) of Mississippi River freshwater thickness and transport in July during the study period. The colors represent the spatial distribution of Mississippi freshwater thickness. The arrows represent the freshwater transport.

[35] The outflow and inflow for the Atchafalaya River freshwater are plotted in Figures 10a and 10b, respectively. For Atchafalaya freshwater, the maximum offshore transport is between 0.07 $m^2\ s^{-1}$ and 0.14 $m^2\ s^{-1}$. The outflow for the Atchafalaya freshwater can occur almost everywhere on the Texas shelf (between 200 km and 800 km in Figure 10), whereas it only takes place in summer months on the Louisiana shelf (between 900 km and 1400 km in Figure 10)

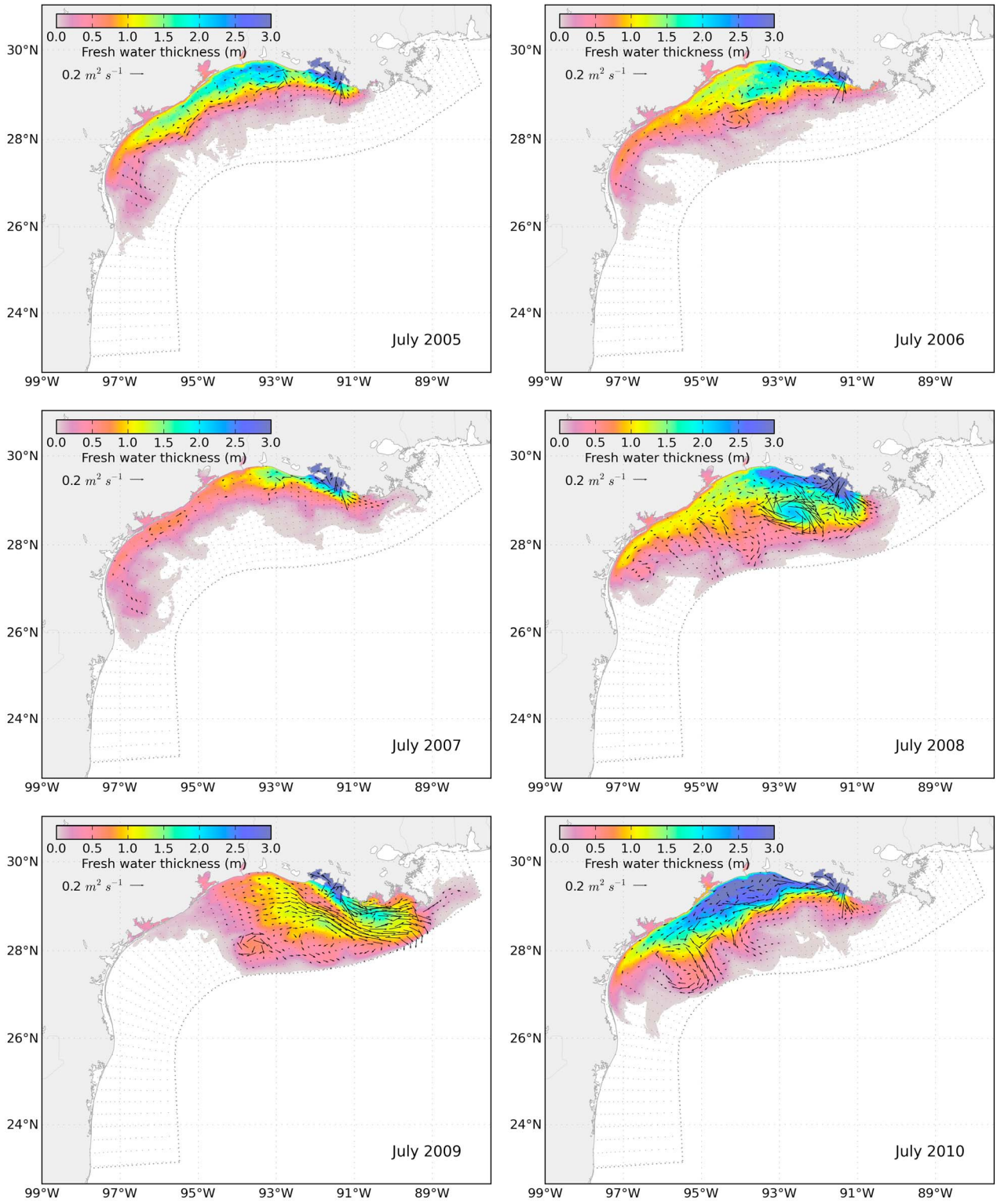

Figure 7. Same as Figure 6 but for Atchafalaya freshwater.

when prevailing wind is upcoast. Offshore transport of Atchafalaya freshwater on the Louisiana shelf is larger from 2008 to 2010 than that from 2005 to 2007. Hot spots for offshore transport on the Texas shelf also show similar propagation trend in the summer months as seen for Mississippi freshwater. The maximum inflow is about half of the outflow (Figure 10). It mainly occurs on the Texas shelf between 400 km and 800 km, and it is more sporadic on the Louisiana shelf.

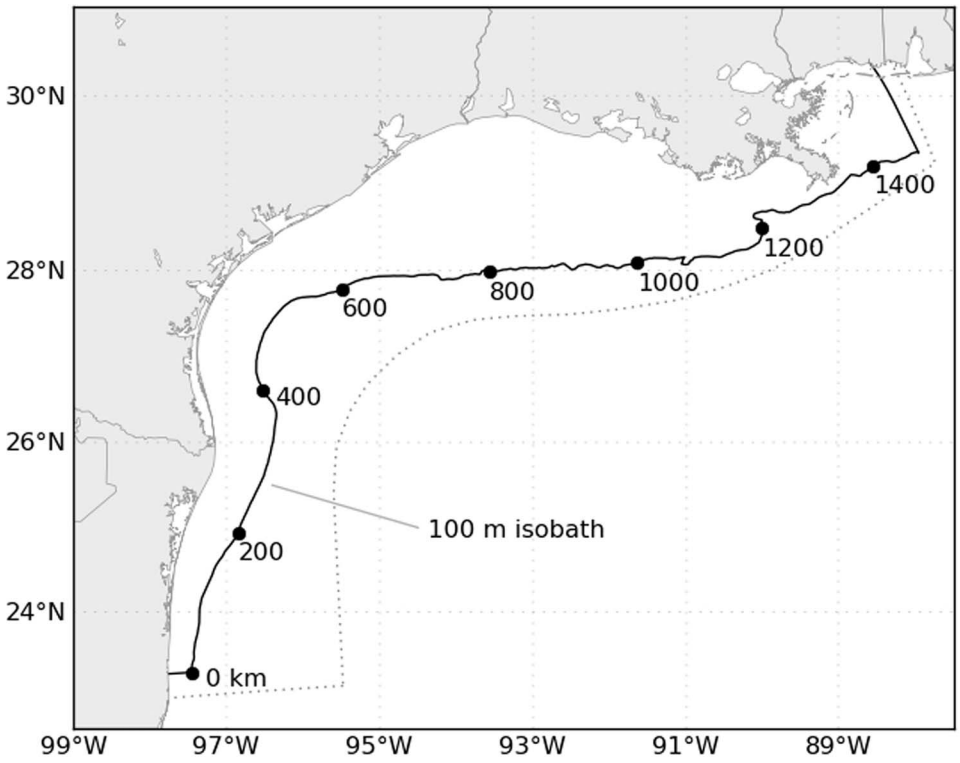

Figure 8. The shelf domain is defined as the region enclosed by the 100-m isobath, and the along-shore limit of the entire model domain The 100-m isobath is highlighted with along-isobath distance indicated. The distance is in km. Note: two margins are removed near the eastern and western boundaries to avoid the influence of the open-boundary nudging to HYCOM.

[36] A question to consider is how much of the river discharged freshwater leaves the western and eastern boundaries of our domain. To quantify this, we define the western and eastern boundaries of our domain 10 grid cells inside of the real boundaries to exclude the nudging area (Figure 8). These figures are not shown but major results of outflow and inflow for these two boundaries are summarized here. The maximum outflow at the western boundary is $\sim 5 \times 10^{-3}$ m^2 s^{-1}, which

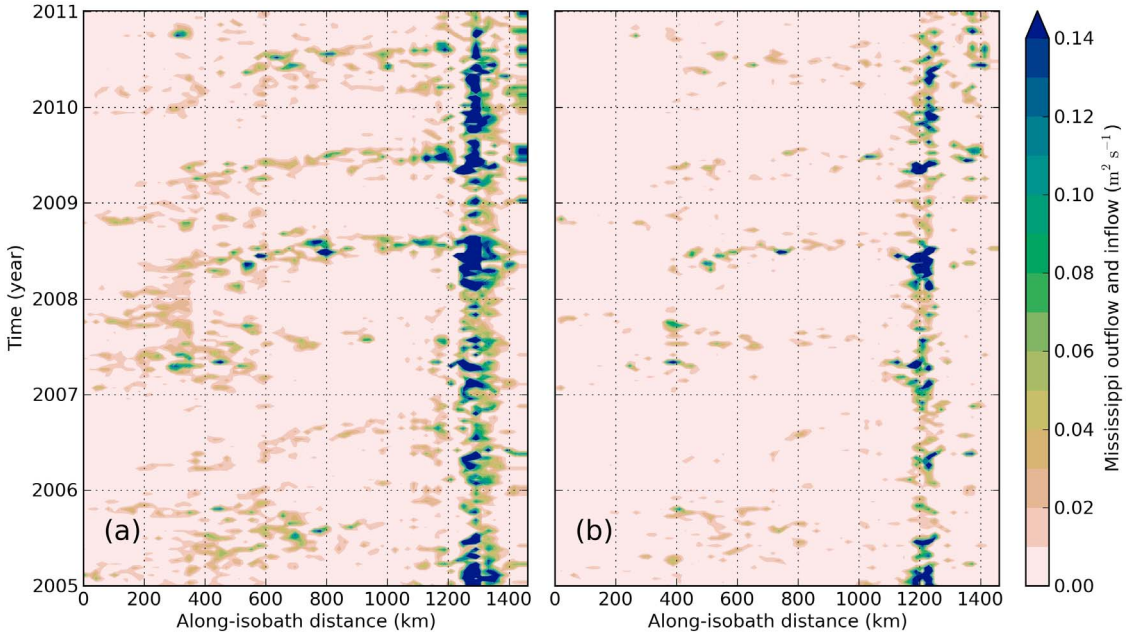

Figure 9. (a) Mississippi freshwater outflow across the 100 m isobath as a function of along-isobath distance and time. (b) Same as Figure 9a but for inflow.

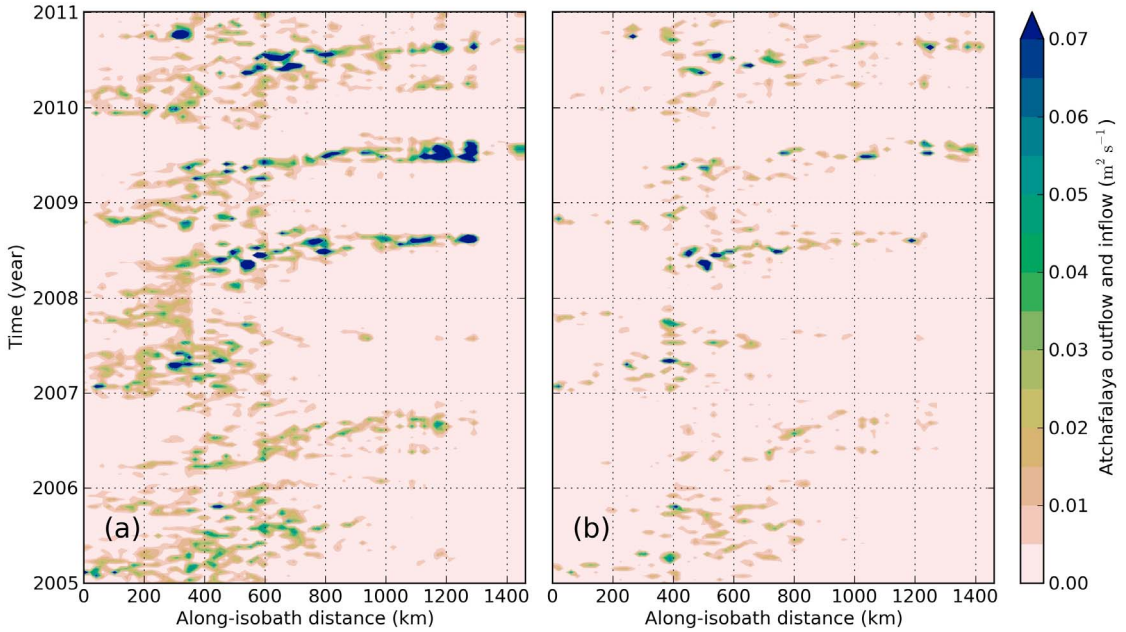

Figure 10. (a) Atchafalaya freshwater outflow across the 100 m isobath as a function of along-isobath distance and time. (b) Same as Figure 10a but for inflow.

is ~2% of the maximum outflow through the southern boundary and the transport near the Mississippi River mouth (Figure 4). The maximum outflow near the western boundary occurs between the 50-m and 100-m isobaths. The inflow through the western boundary is about half of the outflow. The outflow and inflow through the eastern boundary can reach ~0.07 m^2 s^{-1}, and are on the same order as the westward freshwater transport near the river mouth (Figure 4). The maximum outflow at the eastern boundary occurs between the 40-m and 100-m isobaths.

4.3. Filling and Flushing Times

[37] The total freshwater volume V in the shelf domain, bounded offshore by the 100 m isobath, for each river is defined as

$$V_m(t) = \iiint_{shelf} dye_m(x,y,z,t)dxdydz. \tag{6}$$

[38] The filling time for the river-discharged freshwater $\phi_m(t)$ is defined as

$$\phi_m(t) = \frac{V_m(t)}{R_m(t)}, \tag{7}$$

where R is the river discharge to the shelf.

[39] The flushing time for the river-discharged freshwater $\varphi_m(t)$ is defined as

$$\varphi_m(t) = \frac{V_m(t)}{F_m(t)}, \tag{8}$$

where F is the river freshwater transport integrated along the shelf boundary defined in Figure 8. Thus, the flushing time and filling time are similar, with the only difference being that the filling time uses the inflow flux of fresh water from the river, and the flushing time uses the outflow flux of fresh water out of the domain.

[40] In order to determine the timescales of the processes responsible for exporting freshwater from the shelf (F term in equation (8)), a Reynolds decomposition is also performed on the freshwater flux out of the domain. The velocity perpendicular to the shelf boundary and dye are both decomposed as $u = \langle u\rangle + u'$ and $dye = \langle dye\rangle + dye'$, respectively. The time averaging operator is defined as

$$\langle \bullet \rangle = \frac{1}{T}\int_{t-T}^{t} \bullet \, dt, \tag{9}$$

where T is the averaging time scale (e.g., 10 days). Because the time average of mean and perturbation products is zero, e.g., $\langle\langle u\rangle\, dye'\rangle = 0$, the decomposed freshwater flux has only two nonzero terms

$$\iint \langle u\, dye\rangle ds = \iint \langle u' dye'\rangle ds + \iint \langle u\rangle\langle dye\rangle ds, \tag{10}$$

where $\iint \langle u\, dye\rangle ds$, $\iint \langle u' dye'\rangle ds$, and $\iint \langle u\rangle\langle dye\rangle ds$ represent the total freshwater flux, perturbation freshwater flux, and mean freshwater flux across the shelf boundary, respectively (ds represents area integral along the shelf boundary).

[41] The contribution of high frequency motions to the total freshwater flux out of the domain is defined as

$$High\ \ frequency\ \ contribution = \frac{\iint \langle u' dye'\rangle ds}{\iint \langle u dye\rangle ds}. \tag{11}$$

[42] In this section, the contribution of different timescales to the total freshwater flux out of the domain will also be addressed. Note that these definitions (equations (9)–(11))

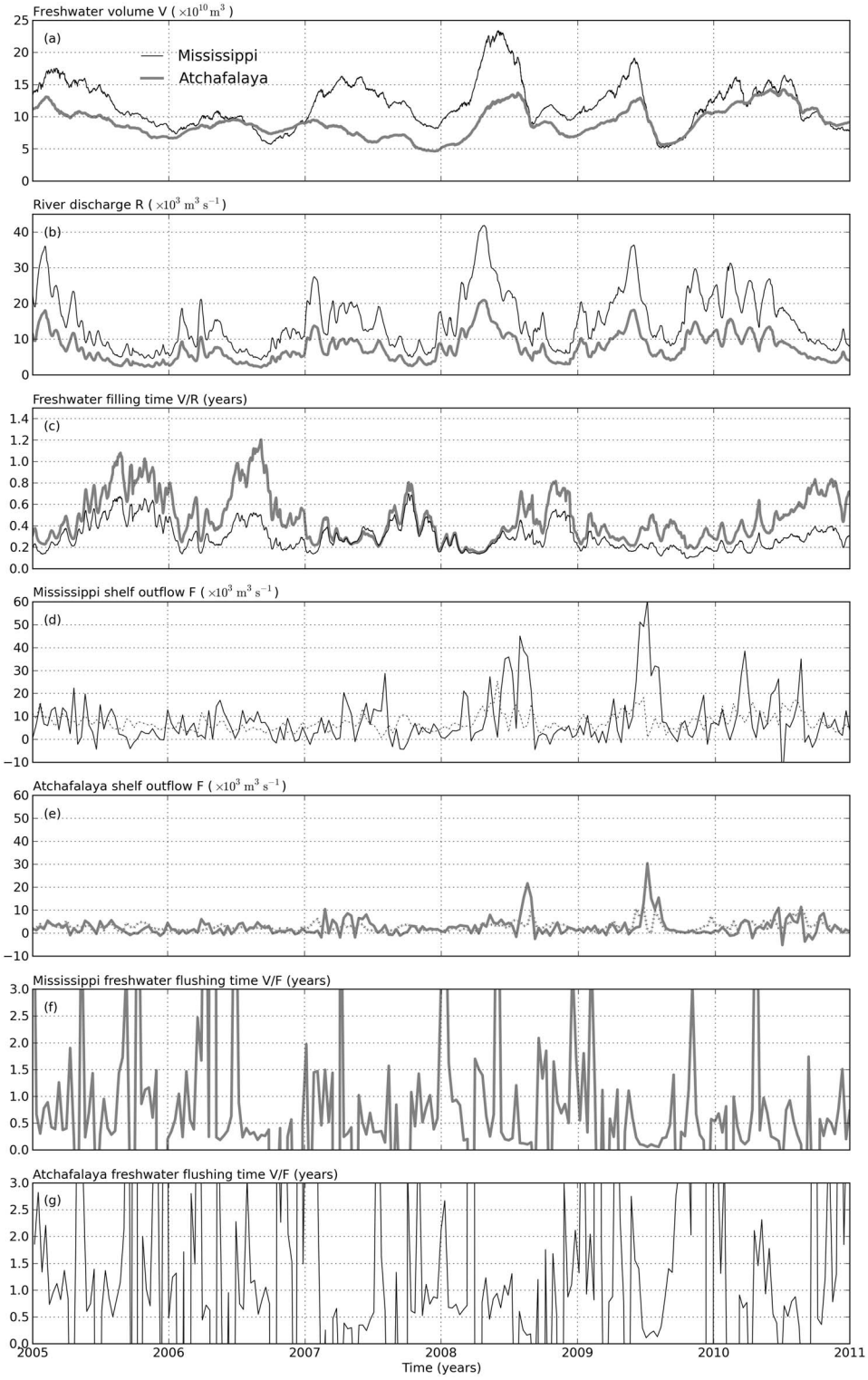

Figure 11. (a) Mississippi (thin black) and Atchafalaya (dark gray) freshwater volume on the Texas-Louisiana shelf. (b) Mississippi and Atchafalaya river discharge time series. (c) Mississippi and Atchafalaya river-discharged freshwater filling time. (d) Mississippi freshwater outflow through the shelf boundary defined in Figure 8. The thin black line represents the mean outflow with an averaging timescale of 10 days based on equations (9) and (10). The dotted black line represents the perturbation outflow with the same average timescale. (e) Same as Figure 11d but for Atchafalaya River. (f) Mississippi river-discharged freshwater flushing time. Flushing time when F is negative is disregarded. Flushing time longer than 3-years is clipped (occurs when F is small and negligible). (g) Same as Figure 11f but for Atchafalaya River.

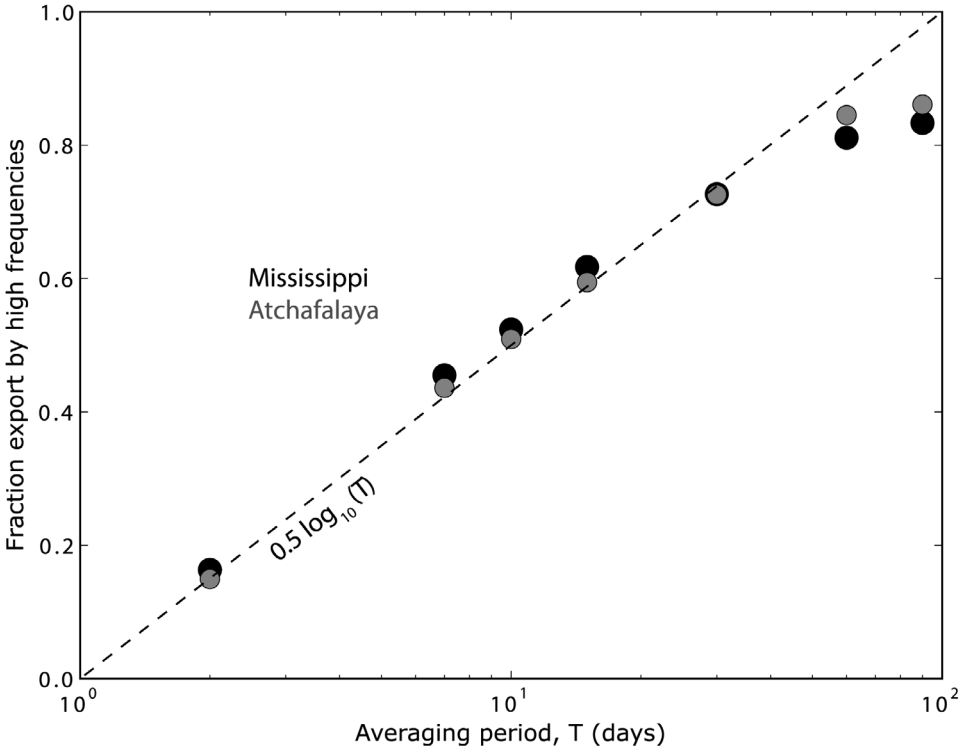

Figure 12. Fraction of the total fresh water export out of the shelf domain by high frequencies as a function of the Reynolds averaging period T. The dashed line represents an empirical fit to the lower section of the data range, averaging periods less than 100 days.

depend on the averaging timescale, T, and the perturbation and mean fluxes are calculated for a range of timescales.

[43] The volume of freshwater, river discharge rate and filling time on the Texas-Louisiana Shelf during the period of 2005 to 2010 for the Mississippi and Atchafalaya Rivers are calculated and plotted in Figures 11a–11c, respectively. All of these parameters show clearly both seasonal and interannual variability. From Figure 11b, we can see the river discharge peaks in April or May in spring during each year (except 2005 when it peaked in early February). The river discharge was high in 2005, 2008 and 2009; while relatively small in 2006, 2007, and 2010. The freshwater volume on the Texas-Louisiana Shelf is correlated with the river discharge, i.e., high discharge means large volume and vice versa (Figure 11a). Maximum correlation between the Mississippi discharge and the Mississippi freshwater volume is 0.75, which occurs with a lag of 3 weeks (discharge leads volume). While for Atchafalaya, maximum correlation is 0.65 with a 33-day lag. Both correlation coefficients are larger than the 99% significance levels. This indicates that inflow and outflow of fresh water on the shelf are approximately correlated as well. If the outflow was constant, for example, we would expect the volume time series to be in quadrature with the river discharge. However, the lag between the peak of the discharge and the peak of the volume indicates that it takes approximately one-month for the river-discharged freshwater to reach the mid-continental shelf and interact with the shelf edge for possible export.

[44] The filling times for both rivers peak in summer (Figure 11c). This is a consequence of high freshwater volume and low river discharge in the summer months. The filling time for Mississippi River in summer is ~7–8 months from 2005 to 2008, and ~4 months in 2009 and 2010. The filling time for Atchafalaya River in summer is ~13 months in 2005 and 2006, ~9 months in 2007, 2008 and 2010, and ~6 months in 2009. It is interesting to note that the minimum summer filling time occurred in a flooding year 2009. As stated before, in 2009, the upcoast wind persisted much longer than climatology, which moved a significant amount of freshwater off the shelf. Thus, the low filling time may be attributed both to a large discharge and a low freshwater volume due to enhanced offshore export. The filling time calculated here is consistent with the significant offshore flow in summer 2009 as shown in Figure 6. The filling times for both rivers are usually shorter in the non-summer months, when the prevailing wind is downcoast and freshwater volume is smaller. Minimum filling times for Mississippi and Atchafalaya are ~2 months and both occur in winter (Figure 11c).

[45] The integrated freshwater transports across the shelf boundary (F) for the Mississippi and Atchafalaya Rivers are plotted in Figures 11d and 11e, respectively. In Figures 11d and 11e, both mean (solid lines) and perturbation (dotted lines) fluxes are shown based on a 10-day averaging timescale (equations (9)–(11)). In Figures 11d and 11e, positive values mean offshore transport, and negative values mean onshore. Figure 11d shows the magnitude of the shelf outflow for Mississippi peaks in spring and summer, and is smaller in fall and winter. The pattern for shelf outflow is correlated with freshwater volume on the shelf and river discharge (Figures 11a, 11b, 11d, and 11e). However, the peaks in the freshwater outflow (F) lag those of the

freshwater volume by about one month (e.g., Figures 11a and 11d). This lag is most apparent in years 2008 and 2009. In the meantime, the shelf outflow seems not directly related to the seasonal wind reversal, which typically occurs in June. (Note that while there is no clear seasonal pattern in the integrated offshore freshwater transport, there are clearly local effects as shown in Figures 9 and 10.) Figure 11d also shows the shelf outflow of the Mississippi freshwater is noisier than the freshwater volume and river discharge. It is interesting to note that the peaks of the perturbation flux in the shelf outflow line up with the peaks of the mean flux. The maximum Mississippi outflow occurred in 2009, consistent with Figure 6. For the Atchafalaya River, the outflow (F) displays similar patterns as the Mississippi River however with smaller magnitude (Figure 11e).

[46] The flushing time for the river discharged freshwater on the Texas-Louisiana Shelf is calculated based on equation (8), using the freshwater volume on the shelf and mean freshwater flux out of the domain (solid lines in Figures 11d and 11e), and it is plotted in Figures 11f and 11g. The flushing time is not calculated when the instant integrated mean freshwater transport is onshore (negative values in Figure 11d). The flushing time is also clipped occasionally when it is larger than 3-years because of the small and negligible shelf outflow. From Figure 11f, we can see that the flushing time for Mississippi is usually less than 1-year, and comparable to the Mississippi freshwater filling time (Figure 11c). The minimum flushing time for Mississippi freshwater occurs in summer when the freshwater volume is small on the shelf and the outflow is large. Also, the flushing time for Mississippi shows less seasonality than the filling time, and there are spikes in the flushing time in the range of 2$\sim$3 years which occur in the case of small outflow (F). The flushing time for the Atchafalaya River (Figure 11g) is longer than Mississippi because the freshwater from Atchafalaya stays on the inner shelf most of the time and has fewer interactions with the shelf boundary (Figure 5).

[47] Figure 12 shows the high-frequency contribution to the total fresh water flux out of the domain as defined in equation (11) for a particular timescale. The line shown on the figure is an empirical fit to the lower section of the data range. This fit indicates that the percentage of fresh water export associated with high-frequency variability is proportional to the logarithm of the averaging period used. This logarithmic proportionality means that the percentage of total fresh water export due to processes acting in, say, the 2–4 day range carry as much fresh water offshore as processes in the 4–8, 8–16, and 16–32 day ranges. Perturbation and mean export are nearly equal when using an averaging period of about 10 days. Note, this is the averaging period used to show the decomposition of the fresh water flux out of the domain in Figure 11.

5. Discussion

[48] This paper has demonstrated several key aspects about the riverine fresh water budget for the Texas-Louisiana Shelf. The first feature to note is that the Mississippi and Atchafalaya plumes occupy different locations on the continental shelf, although there is certainly some overlap. These plumes are difficult to differentiate using salinity alone, because there is no observational evidence for a distinct salinity signal for either plume. However, using a dye tracer, in the context of a numerical circulation model, the different regions occupied by the two plumes can be clearly seen. Freshwater from the Mississippi does not appear to interact strongly with the coast, except in the region very near the Mississippi River Delta. Freshwater from the Atchafalaya lies between the Mississippi river water and the coast for much of the domain. As such, it is the Mississippi River water, occupying the region seaward of the Atchafalaya water that interacts more strongly with the shelf edge. Consequently, the Mississippi River water has a shorter filling time on the shelf, relative to Atchafalaya River water, despite having a larger integrated fresh water volume. Because the ratio of Atchafalaya to Mississippi discharge is mandated to be approximately 1:2, changes to this ratio can have profound implications for the hydrography of the Texas-Louisiana Shelf [*Bianchi et al.*, 2010].

[49] Patterns of export are also different. The Mississippi has two primary export pathways, one near the Mississippi River Delta, and one along the western section of the Texas-Louisiana Shelf. Atchafalaya water, isolated from the shelf edge by the Mississippi River water, is primarily exported at the end of the southwestern edge of the plume, or the downcoast reach of the plume. The downcoast extent of the plume shifts as the seasonal winds shift. The winds are generally onshore (toward Texas) in spring and summer, and shift slightly from being more easterly to more southerly. Because the coastline is curved, there is an upcoast flow where the winds are upwelling, and a downcoast flow where the winds are downwelling. Winds switch from downwelling to upwelling first along the southern TX coast, and this point moves upcoast over the season. This is the point, with the convergent winds and convergent flow driven by those winds [*Morey et al.*, 2003; *Zhang and Hetland*, 2012], where the offshore transport of fresh water occurs. This point shifts upcoast as the winds shift, and the shift can be clearly seen in Figures 9 and 10.

[50] The freshwater export through the western and eastern boundaries of the model domain is also quantified. The maximum outflow at the western boundary is only $\sim$2% of the maximum outflow through the 100-m isobath of the shelf domain. The outflow through the eastern boundary are about the same order as the westward freshwater transport near the river mouth, supporting *Dinnel and Wiseman*'s [1986] assertion that $\sim$50% of the Mississippi discharged freshwater is transported onto the Texas-Louisiana Shelf.

[51] The percent of fresh water flux out of the shelf domain is a regular function of the averaging period and indicates that there is no single process that is responsible for exporting water from the shelf. If the fresh water flux was primarily caused by some individual process, we should expect to see a more pronounced peak in this curve associated with the spectral peak of energy for that process, but this is not the case. It seems that a very wide range of processes control the export of fresh water from the shelf. This is also suggested in Figures 9 and 10, which clearly show multiple hot spots of export, where different identified processes control the export.

[52] There is significant interannual variability in the amount of riverine fresh water on the shelf. This is primarily related to the magnitude of the annual freshet, as is clear from the strong positive correlation between river discharge

and fresh water volume on the shelf. However, as seen in the case of 2009, this can be modulated somewhat by the strength and duration of the summertime upwelling winds. Both river discharge and wind stress are correlated with the areal extent of seasonal hypoxia, so we expect that both of these factors will influence circulation and shelf ecosystem processes.

6. Conclusions

[53] This paper investigates the transport, filling and flushing times of freshwater introduced from the Mississippi and Atchafalaya Rivers on the Texas-Louisiana shelf with a high-resolution coastal model of circulation. It is the first attempt to treat the Mississippi and Atchafalaya freshwater individually using numerical dyes. Both the climatological and interannual variability of freshwater characteristics on the Texas-Louisiana Shelf are addressed using the model output from 2005 to 2010, when the model salinity field has reached equilibrium.

[54] The seasonal patterns of Mississippi and Atchafalaya freshwater transport are consistent with the prevailing winds, but with significant interannual variability. In the non-summer months, the major freshwater transport is downcoast and occurs mainly in a narrow band inside of 20 m isobath. Maximum freshwater transport occurs between 10- and 20-m isobaths for Mississippi, while between the coast and 10-m isobath for Atchafalaya. Non-summer freshwater transport is larger in winter and spring than in fall. In summer, the transport decreases dramatically near the coast due to the competing effect of downcoast-propagating freshwater and upcoast wind-driven flow. The freshwater transport is upcoast on the mid shelf with offshore component, consistent with the Ekman transport. Maximum offshore transport occurs on the mid Louisiana Shelf in July and August.

[55] We define the Texas-Louisiana Shelf domain as the region enclosed by the 100-m isobaths, and the along-shore limit of the entire model domain, approximately from the Louisiana-Mississippi border to the Texas-Mexico border. The freshwater flux out of this domain is quantified, and hot spots for outflow and inflow along the 100-m isobath are identified. A Reynolds decomposition of the freshwater export out of the shelf domain suggests that there is no single process that is responsible for exporting water from the shelf. Most of the export occurs with timescales of less than 100 days, while perturbation and mean export are nearly equal when using an averaging period of about 10 days.

[56] The filling and flushing times for river discharges on the shelf are estimated based on freshwater volume, discharge rate, and shelf outflow. Freshwater volume on the shelf lags the discharge by about 3 weeks for Mississippi and 33 days for Atchafalaya. Filling times, based on the river discharge, range from ~3 months in the non-summer months to ~6 months in summer for Mississippi, while for Atchafalaya from ~3–4 months to ~1 year. The filling time for Mississippi River is smaller than Atchafalaya despite the larger volume on the shelf. This is caused by the location of the Mississippi plume, which lies seaward of the Atchafalaya plume and thus has more interactions with the shelf boundaries. Flushing times, based on the fresh water flux out of the shelf domain, are more variable. They range from several months to several years, and display less seasonality. Increased knowledge of the river-discharged freshwater characteristics investigated in this paper provides insight to help improve our understanding of the ecosystem processes on the Texas-Louisiana Shelf.

[57] **Acknowledgments.** This study is funded by the Texas General Land Office under contracts 08-054-000-1146 and 10-096-000-3927 and by the NOAA Center for Sponsored Coastal Ocean Research under contract NA09NOS4780208. Numerical simulations were performed on the supercomputer at the Supercomputing Facility at TAMU. MCH hydrographic data used in this paper are available through the National Oceanographic Data Center (http://nodc.noaa.gov) under project accession code 88164. We also thank two anonymous reviewers for their valuable comments and suggestions.

References

Barth, A., A. Alvera-Azcarate, and R. H. Weisberg (2008), Benefit of nesting a regional model into a large-scale ocean model instead of climatology. Application to the West Florida Shelf, *Cont. Shelf Res.*, *28*, 561–573, doi:10.1016/j.csr.2007.11.004.

Bianchi, T. S., S. F. DiMarco, J. H. Cowan Jr., R. D. Hetland, P. Chapman, J. W. Day, and M. A. Allison (2010), The science of hypoxia in the northern Gulf of Mexico: A review, *Sci. Total Environ.*, *408*(7), 1471–1484, doi:10.1016/j.scitotenv.2009.11.047.

Bogden, P. S., P. Malanotte-Rizzoli, and R. P. Signell (1996), Open-ocean boundary conditions from interior data: Local and remote forcing of Massachusetts Bay, *J. Geophys. Res.*, *101*, 6487–6500, doi:10.1029/95JC03705.

Chapman, D. C. (1985), Numerical treatment of cross-shelf open boundaries in a barotropic coastal ocean model, *J. Phys. Oceanogr.*, *15*, 1060–1075, doi:10.1175/1520-0485(1985)015<1060:NTOCSO>2.0.CO;2.

Cho, K., R. O. Reid, and W. D. Nowlin Jr. (1998), Objectively mapped stream function fields on the Texas-Louisiana Shelf based on 32 months of moored current meter data, *J. Geophys. Res.*, *103*(C5), 10,377–10,390, doi:10.1029/98JC00099.

Cochrane, J. D., and F. J. Kelly (1986), Low-frequency circulation on the Texas-Louisiana Continental Shelf, *J. Geophys. Res.*, *91*(C9), 10,645–10,659, doi:10.1029/JC091iC09p10645.

Dale, V., et al. (2008), Hypoxia in the northern Gulf of Mexico: An update by the EPA Science Advisory Board, U.S. Environ. Prot. Agency, Washington, D. C.

DiMarco, S. F., and R. O. Reid (1998), Characterization of the principal tidal current constituents on the Texas-Louisiana Shelf, *J. Geophys. Res.*, *103*(C2), 3093–3109, doi:10.1029/97JC03289.

DiMarco, S. F., M. K. Howard, and R. O. Reid (2000), Seasonal variation of wind-driven diurnal current cycling on the Texas-Louisiana continental shelf, *Geophys. Res. Lett.*, *27*, 1017–1020, doi:10.1029/1999GL010491.

DiMarco, S. F., P. Chapman, N. Walker, and R. D. Hetland (2010), Does local topography control hypoxia on the eastern Texas-Louisiana Shelf?, *J. Mar. Syst.*, *80*, 25–35, doi:10.1016/j.jmarsys.2009.08.005.

Dinnel, S. P., and W. J. Wiseman Jr. (1986), Fresh water on the Louisiana and Texas Shelf, *Cont. Shelf Res.*, *6*(6), 765–784, doi:10.1016/0278-4343(86)90036-1.

Etter, P. C., M. K. Howard, and J. D. Cochrane (2004), Heat and freshwater budgets of the Texas-Louisiana Shelf, *J. Geophys. Res.*, *109*, C02024, doi:10.1029/2003JC001820.

Feng, Y., S. F. DiMarco, and G. A. Jackson (2012), Relative role of wind forcing and riverine nutrient input on the extent of hypoxia in the northern Gulf of Mexico, *Geophys. Res. Lett.*, *39*, L09601, doi:10.1029/2012GL051192.

Flather, R. A. (1976), A tidal model of the northwest European continental shelf, *Mem. Soc. R. Sci. Liege*, *10*(6), 141–164.

Forrest, D. R., R. D. Hetland, and S. F. DiMarco (2011), Multivariable statistical regression models of the areal extent of hypoxia over the Texas-Louisiana continental shelf, *Environ. Res. Lett.*, *6*, 045002, doi:10.1088/1748-9326/6/4/045002.

Galperin, B., L. H. Kantha, and A. Rosati (1988), A quasi-equilibrium turbulent energy model for geophysical flows, *J. Atmos. Sci.*, *45*, 55–62, doi:10.1175/1520-0469(1988)045<0055:AQETEM>2.0.CO;2.

Haidvogel, D. B., H. G. Arango, K. Hedstrom, A. Beckmann, P. Malanotte-Rizzoli, and A. F. Shchepetkin (2000), Model evaluation experiments in the North Atlantic Basin: Simulations in nonlinear terrain-following coordinates, *Dyn. Atmos. Oceans*, *32*, 239–281, doi:10.1016/S0377-0265(00)00049-X.

Hetland, R. D. (2006), Event-driven model skill assessment, *Ocean Modell.*, *11*(1–2), 214–223, doi:10.1016/j.ocemod.2004.12.001.

Hetland, R. D., and L. Campbell (2007), Convergent blooms of *Karenia brevis* along the Texas coast, *Geophys. Res. Lett.*, *34*, L19604, doi:10.1029/2007GL030474.

Hetland, R. D., and S. F. DiMarco (2008), How does the character of oxygen demand control the structure of hypoxia on the Texas-Louisiana continental shelf?, *J. Mar. Syst.*, *70*, 49–62, doi:10.1016/j.jmarsys.2007.03.002.

Hetland, R. D., and S. F. DiMarco (2012), Skill assessment of a hydrodynamic model of circulation over the Texas-Louisiana continental shelf, *Ocean Modell.*, *43–44*, 49–62, doi:10.1016/j.ocemod.2011.11.009.

Ichiye, T. (1960), On the hydrography near Mississippi Delta, *Oceanogr. Mag.*, *11*(2), 65–78.

Johnson, D. R., T. P. Boyer, H. E. Garcia, R. A. Locarnini, O. K. Baranova, and M. M. Zweng (2009), World Ocean Database 2009 documentation, edited by S. Levitus, *NODC Internal Rep. 20*, 175 pp., NOAA Print. Off., Silver Spring, Md.

Liu, Y., P. MacCready, B. M. Hickey, E. P. Dever, P. M. Kosro, and N. S. Banas (2009), Evaluation of a coastal ocean circulation model for the Columbia River plume in summer 2004, *J. Geophys. Res.*, *114*, C00B04, doi:10.1029/2008JC004929.

Marchesiello, P., J. C. McWilliams, and A. Shchepetkin (2003), Equilibrium structure and dynamics of the California current system, *J. Phys. Oceanogr.*, *33*, 753–783.

Meade, R. H. (1996), *River-Sediment Inputs to Major Deltas*, Kluwer Acad., Dordrecht, Netherlands.

Mellor, G. L., and T. Yamada (1974), A hierarchy of turbulent closure models for planetary boundary layers, *J. Atmos. Sci.*, *31*, 1791–1806, doi:10.1175/1520-0469(1974)031<1791:AHOTCM>2.0.CO;2.

Milliman, J. D., and R. H. Meade (1983), World-wide delivery of river sediment to the ocean, *J. Geol.*, *91*(1), 1–21, doi:10.1086/628741.

Morey, S. L., P. J. Martin, J. J. O'Brien, A. A. Wallcraft, and J. Zavala-Hidalgo (2003), Export pathways for river discharged fresh water in the northern Gulf of Mexico, *J. Geophys. Res.*, *108*(C10), 3303, doi:10.1029/2002JC001674.

Nowlin, W. D., Jr., A. E. Jochens, R. O. Reid, and S. F. DiMarco (1998), Texas-Louisiana Shelf circulation and transport processes study: Synthesis report, vol. 1, Technical report, *OCS Study MMS 98-0035*, 502 pp., Gulf of Mex. OCS Reg., Miner. Manage. Serv., U.S. Dep. of the Int., New Orleans, La.

Nowlin, W. D., Jr., A. E. Jochens, S. F. DiMarco, R. O. Reid, and M. K. Howard (2005), Low-frequency circulation over the Texas-Louisiana continental shelf, in *Circulation in the Gulf of Mexico: Observations and Models*, *Geophys. Monogr. Ser.*, vol. 161, edited by W. Sturges and A. Lugo-Fernandez, pp. 219–240, AGU, Washington, D. C., doi:10.1029/161GM17

Ohlmann, J., P. Niiler, C. Fox, and R. Leben (2001), Eddy energy and shelf interactions in the Gulf of Mexico, *J. Geophys. Res.*, *106*(C2), 2605–2620, doi:10.1029/1999JC000162.

Shchepetkin, A. F., and J. C. McWilliams (2005), The Regional Oceanic Modeling System (ROMS): A split-explicit, free-surface, topographically following-coordinate oceanic model, *Ocean Modell.*, *9*, 347–404, doi:10.1016/j.ocemod.2004.08.002.

Wang, L., and D. Justic (2009), A modeling study of the physical processes affecting the development of seasonal hypoxia over the inner Louisiana-Texas Shelf: Circulation and stratification, *Cont. Shelf Res.*, *29*, 1464–1476, doi:10.1016/j.csr.2009.03.014.

Warner, J. C., W. R. Geyer, and J. A. Lerczak (2005), Numerical modeling of an estuary: A comprehensive skill assessment, *J. Geophys. Res.*, *110*, C05001, doi:10.1029/2004JC002691.

Zhang, X., S. F. DiMarco, D. C. Smith IV, M. K. Howard, A. E. Jochens, and R. D. Hetland (2009), Near-resonant response to sea breeze on a stratified continental shelf, *J. Phys. Oceanogr.*, *39*, 2137–2155, doi:10.1175/2009JPO4054.1.

Zhang, X., D. C. Smith IV, S. F. DiMarco, and R. D. Hetland (2010), A numerical study of sea-breeze-driven ocean Poincare wave propagation and mixing near the critical latitude, *J. Phys. Oceanogr.*, *40*, 48–66, doi:10.1175/2009JPO4216.1.

Zhang, X., M. Marta-Almeida, and R. D. Hetland (2012), A high-resolution pre-operational forecast model of circulation on the Texas-Louisiana continental shelf and slope, *J. Oper. Oceanogr.*, *5*, 19–34.

Zhang, Z., and R. D. Hetland (2012), A numerical study on convergence of along-shore flows over the Texas-Louisiana Shelf, *J. Geophys. Res.*, doi:10.1029/2012JC008145, in press.